

THE MARCONI REVIEW

Volume XXIII Number 139 Fourth Quarter 1960

The Marconi Review is published four times a year

Annual subscription £1. Single copies 5s. Postage paid to any part of the world

Copyright reserved by Marconi's Wireless Telegraph Company Limited, Chelmsford, Essex, England

EDITOR L. E. Q. WALKER A.R.C.S.

Marconi's Wireless Telegraph Company Limited, Baddow Research Laboratories
West Hanningfield Road, Great Baddow, Essex, England

The Effect of Mixing Two Noisy Signals

By N. A. HUTTLY, M.Sc.

A problem which often arises in the field of radio is that of determining the signal/noise ratio of the beat note obtained from mixing together two noisy signals. In the case where one signal only is noisy and where the bandwidth of the beat note is much smaller than that of the noisy input signal, the effect of mixing is one of linearity in that the overall bandwidth is equal to that around the beat note. One would expect however, that there would be some departure from linearity if both signals contain noise and it is the purpose of this article to investigate this question.

The first section of the article will give the general analytical solution to the problem. The second section will deal with a special case which occurs frequently in practice, that of a single tuned circuit and the third section will give approximate solutions when certain assumptions about the various bandwidths and the beat note frequency have been made.

General Analytical Solution

When considering problems dealing with signals and their attendant noise, the course is made to statistical theory, in particular to that part of it dealing with stochastic time-series. This means that the answers to these problems are quoted in statistical terms and use is made of the expression signal/noise ratio, defined as the ratio of the signal output to the r.m.s. (or standard deviation) of the noise output. In what follows, therefore, the question of mixing noise signals in these terms will be discussed, and

the problem under consideration can be described as a comparison of the signal/noise ratio before mixing to that after mixing.

Let us therefore, consider two input voltages V_1, V_2 consisting of signal plus noise; they can be represented as

$$V_1 = S_1 \cos \omega_1 t + X_1 \cos \omega_1 t + Y_1 \sin \omega_1 t \quad (1)$$

$$V_2 = S_2 \cos \omega_2 t + X_2 \cos \omega_2 t + Y_2 \sin \omega_2 t \quad (2)$$

Where S_1, S_2 are the signal amplitudes

X_1, X_2 are the noise amplitudes in phase with the signal

Y_1, Y_2 are the noise amplitudes in quadrature with the signal

($X_1 \dots Y_2$ are all functions of time, i.e. $X_1 = X_1(t)$ etc.)

and ω_1, ω_2 are the input signal frequencies.

These two input voltages are mixed by first multiplying them together and then passing the product through a band-pass filter. Thus we shall have

$$\begin{aligned} W &= V_1 V_2 \\ &= (S_1 \cos \omega_1 t + X_1 \cos \omega_1 t + Y_1 \sin \omega_1 t) (S_2 \cos \omega_2 t + X_2 \cos \omega_2 t + Y_2 \sin \omega_2 t) \\ &= S_1 S_2 \cos \omega_1 t \cos \omega_2 t + X_1 S_2 \cos \omega_1 t \cos \omega_2 t + S_2 Y_1 \sin \omega_1 t \cos \omega_2 t \\ &+ X_2 S_1 \cos \omega_1 t \cos \omega_2 t + X_1 X_2 \cos \omega_1 t \cos \omega_2 t + X_2 Y_1 \sin \omega_1 t \cos \omega_2 t \\ &+ Y_2 S_1 \cos \omega_1 t \sin \omega_2 t + Y_2 X_1 \cos \omega_1 t \sin \omega_2 t + Y_1 Y_2 \sin \omega_1 t \sin \omega_2 t \\ &= \frac{1}{2} \left[S_1 S_2 (\cos \omega_1 - \omega_2 t + \cos \overline{\omega_1 + \omega_2} t) \right. \\ &+ X_1 S_2 (\cos \omega_1 - \omega_2 t + \cos \overline{\omega_1 + \omega_2} t) \\ &+ S_2 Y_1 (\sin \omega_1 - \overline{\omega_2} t + \sin \overline{\omega_1 + \omega_2} t) \\ &+ X_2 S_1 (\cos \overline{\omega_1 - \omega_2} t + \cos \overline{\omega_1 + \omega_2} t) \\ &+ X_1 X_2 (\cos \omega_1 - \omega_2 t + \cos \overline{\omega_1 + \omega_2} t) \\ &+ X_2 Y_1 (\sin \overline{\omega_1 - \omega_2} t + \sin \overline{\omega_1 + \omega_2} t) \\ &+ Y_2 S_1 (-\sin \overline{\omega_1 - \omega_2} t + \sin \overline{\omega_1 + \omega_2} t) \\ &+ Y_2 X_1 (-\sin \overline{\omega_1 - \omega_2} t + \sin \overline{\omega_1 + \omega_2} t) \\ &\left. + Y_1 Y_2 (\cos \omega_1 - \omega_2 t - \cos \overline{\omega_1 + \omega_2} t) \right] \quad (3) \end{aligned}$$

and on passing this product through a band-pass filter whose impulse response is

$$K(t) \cos \{(\omega_1 - \omega_2 + \delta)t + \varphi\} \quad (4)$$

where

$K(t)$ is the amplitude envelope of the beatnote

δ is the divergence of the natural oscillation of the filter from the beatnote frequency

φ is a phase constant

we get the final output voltage as

$$V = \frac{1}{2} \int_{-\infty}^u K(u-t) \cos \{(\omega_0 + \delta)(u-t) + \varphi\} \tag{6}$$

$$\times \{S_1 S_2 \cos \omega_0 t + X_1 S_2 \cos \omega_0 t + \dots + Y_1 Y_2 \cos \omega_0 t\} dt$$

from (4) and (5), where $\omega_0 = \omega_1 - \omega_2$.

The expression (6) can be split up into two parts where the part containing the term $S_1 S_2 \cos \omega_0 t$ is the signal output and the remainder the noise output.

In order to obtain the signal/noise ratio of the output V it is necessary to investigate its statistical properties, viz., its mean value, or in statistical terms its expected value $E(V)$, and its standard deviation $\sigma(V)$.

We assume that the noise present has zero mean value, so that

$$E(X_1) = E(X_2) = E(Y_1) = E(Y_2) = 0 \tag{7}$$

and we further assume that X_1, Y_1 are Gaussianly distributed variables with standard deviation (s.d) σ_1 ; and X_2, Y_2 are similarly distributed variables with s.d σ_2 .

Since X_1, Y_1 are independent

$$E(X_1 Y_1) = E(X_1)E(Y_1) = 0 \text{ by virtue of (7)}$$

and similarly $E(X_2 Y_2) = 0$.

Finally we assume that V_1 and V_2 are independent voltages so that

$$E(X_1 X_2) = E(Y_1 Y_2) = 0 \tag{8}$$

since the noise voltages are stochastic and continuous in nature, expressions involving the auto-correlation are present in any measurements using these noise voltages; these are taken to have the form

$$\begin{aligned} E\{X_1(t) X_1(t + \tau)\} &= E\{Y_1(t) Y_1(t + \tau)\} = \sigma_1^2 \rho_1(\tau) \\ E\{X_2(t) X_2(t + \tau)\} &= E\{Y_2(t) Y_2(t + \tau)\} = \sigma_2^2 \rho_2(\tau) \end{aligned} \tag{9}$$

this gives the $E(V)_{\text{NOISE}}$ from equation (6) to be

$$\begin{aligned} &\left[\frac{1}{2} \int_{-\infty}^u K(u-t) \cos \{(\omega_0 + \delta)(u-t) + \varphi\} \{X_1 S_2 \cos \omega_0 t + \dots\} dt \right] \\ &\frac{1}{2} \int_{-\infty}^u K(u-t) \cos \{(\omega_0 + \delta)(u-t) + \varphi\} \left[\cos \omega_0 t E(X_1 S_2) + \dots \right] dt \end{aligned}$$

and since S_1, S_2 are not stochastic variables $E(S_2 X_1) = S_2 E(X_1)$, etc.

Therefore $E(V)_{\text{NOISE}} = 0$ by (7) and (8), as would be expected.

The variance or $\sigma^2(V)$ then becomes

$$\begin{aligned} E(V^2)_{\text{NOISE}} &= \frac{1}{4} E \left[\int_{-\infty}^u K(u-t) \cos\{(\omega_0 + \delta)(u-t) + \varphi\} \{X_1 S_2 \cos \omega_0 t + \dots\} dt \right. \\ &= \frac{1}{4} E \left[\int_{-\infty}^u \int_{-\infty}^u K(u-t) K(u-t') \right. \\ &\quad \times \cos\{(\omega_0 + \delta)(u-t) + \varphi\} \cos\{(\omega_0 + \delta)(u-t') + \varphi\} \\ &\quad \times \{ \cos \omega_0 t (X_1 S_2 + X_2 S_1 + X_1 X_2 + Y_1 Y_2) \\ &\quad + \sin \omega_0 t (S_2 Y_1 + X_2 Y_1 - Y_2 S_1 - Y_2 X_1) \} \\ &\quad \times \{ \cos \omega_0 t' (X'_1 S_2 + X'_2 S_1 + X'_1 X'_2 + Y'_1 Y'_2) \\ &\quad + \sin \omega_0 t' (S_2 Y'_1 + X'_2 Y'_1 - Y'_2 S_1 - Y'_2 X'_1) \} dt dt' \end{aligned}$$

(Note: $X = X(t)$ and $X' = X(t')$ etc.)

By writing $t' = t + \tau$ this expression reduces by virtue of (7), (8) and (9)

$$\begin{aligned} E(V^2)_{\text{NOISE}} &= \frac{1}{4} \left[\int_{-\infty}^u \int_{-\infty}^{u-t} K(u-t) K(u-t-\tau) \cos\{(\omega_0 + \delta)(u-t) + \varphi\} \right. \\ &\quad \times \cos\{(\omega_0 + \delta)(u-t-\tau) + \varphi\} \\ &\quad \times [S_1^2 \sigma_2^2 \rho_2(\tau) + S_2^2 \sigma_1^2 \rho_1(\tau) + 2\sigma_1^2 \sigma_2^2 \rho_1(\tau) \rho_2(\tau)] \\ &\quad \times [\cos \omega_0 t \cos \omega_0(t + \tau) + \sin \omega_0 t \sin \omega_0(t + \tau)] dt d\tau \end{aligned} \quad (11)$$

Now $\cos \omega_0 t \cos \omega_0(t + \tau) + \sin \omega_0 t \sin \omega_0(t + \tau) = \cos \omega_0 \tau$
and on putting $u - t = s$, (11) becomes

$$\begin{aligned} & - \frac{1}{4} \int_{-\infty}^0 \int_{-\infty}^s K(s) K(s-\tau) \cos\{(\omega_0 + \delta)s + \varphi\} \cos\{(\omega_0 + \delta)(s-\tau) + \varphi\} \\ & \quad \times \cos \omega_0 \tau \{S_1^2 \sigma_2^2 \rho_2(\tau) + S_2^2 \sigma_1^2 \rho_1(\tau) + 2\sigma_1^2 \sigma_2^2 \rho_1(\tau) \rho_2(\tau)\} ds d\tau \\ & = \frac{1}{4} \int_0^{\infty} K(s) \cos\{(\omega_0 + \delta)s + \varphi\} \\ & \quad \times \left[\int_{-\infty}^s K(s-\tau) \cos \omega_0 \tau \cos\{(\omega_0 + \delta)(s-\tau) + \varphi\} \right. \\ & \quad \times \{S_1^2 \sigma_2^2 \rho_2(\tau) + S_2^2 \sigma_1^2 \rho_1(\tau) + 2\sigma_1^2 \sigma_2^2 \rho_1(\tau) \rho_2(\tau)\} d\tau \end{aligned}$$

or finally if we put $s - \tau = v$,

$E(V^2)_{\text{NOISE}}$ (i.e. square of R.M.S.)

$$\begin{aligned} & = \frac{1}{4} \int_0^{\infty} K(s) \cos\{(\omega_0 + \delta)s + \varphi\} ds \\ & \quad \times \int_0^{\infty} K(v) \cos\{(\omega_0 + \delta)v + \varphi\} \cos\{\omega_0(s-v)\} \{S_1^2 \sigma_2^2 \rho_2(s-v) \\ & \quad + S_2^2 \sigma_1^2 \rho_1(s-v) + 2\sigma_1^2 \sigma_2^2 \rho_1(s-v) \rho_2(s-v)\} dv \end{aligned} \quad (12)$$

Now, to get the signal/noise ratio we need the amplitude of the signal output. This is obtained from the first part of the output voltage given by equation (6) viz.:

$$-\frac{1}{2} \int_{-\infty}^u K(u-t) \cos \{(\omega_0 + \delta)(u-t) + \varphi\} S_1 S_2 \cos(\omega_0 t) dt$$

If we put $u - t = s$ this becomes

$$\begin{aligned} & \frac{S_1 S_2}{2} \int_0^\infty K(s) \cos \{(\omega_0 + \delta)s + \varphi\} \cos \{\omega_0(u-s)\} ds \\ &= \frac{S_1 S_2}{2} \left[\cos(\omega_0 u) \int_0^\infty K(s) \cos \{(\omega_0 + \delta)s + \varphi\} \cos(\omega_0 s) ds \right. \\ & \quad \left. + \sin(\omega_0 u) \int_0^\infty K(s) \cos \{(\omega_0 + \delta)s + \varphi\} \sin(\omega_0 s) ds \right] \end{aligned}$$

from which the amplitude is given by

$$\begin{aligned} & \frac{S_1 S_2}{2} \left\{ \left[\int_0^\infty K(s) \cos \{(\omega_0 + \delta)s + \varphi\} \cos(\omega_0 s) ds \right]^2 \right. \\ & \quad \left. + \left[\int_0^\infty K(s) \cos \{(\omega_0 + \delta)s + \varphi\} \sin(\omega_0 s) ds \right]^2 \right\}^{\frac{1}{2}} \quad (13) \end{aligned}$$

Hence the signal/noise ratio is given by dividing equation (13) by the square root of equation (12).

Case of Single-tuned Circuit

Equation (12) above is the general solution to the problem of mixing two noisy signals but in its present form it is not of much practical use. We shall consider, therefore, the special case of a single-tuned circuit where the filter envelope $K(s)$ and the auto-correlations $\rho_1(\tau)$, $\rho_2(\tau)$ have the particular forms,

$$\left. \begin{aligned} K(s) &= e^{-\beta s} \\ \rho_1(\tau) &= e^{-\alpha_1 \tau} \\ \rho_2(\tau) &= e^{-\alpha_2 \tau} \end{aligned} \right\} \alpha_1, \alpha_2 \text{ \& } \beta > 0 \quad (14)$$

where α_1 , α_2 and β are related to f_1 , f_2 , f_b , the bandwidths between the dB points of the input voltages V_1 , V_2 and the beatnote respectively, by the relations

$$\begin{aligned} \alpha_1 &= \pi f_1 \\ \alpha_2 &= \pi f_2 \\ \beta &= \pi f_B \end{aligned}$$

(N.B. We shall now assume that the bandwidths are centred on the frequencies ω_1 , ω_2 and $\omega_0 + \delta$.)

We shall therefore obtain the expression for the variance of the output noise by substituting (14) into (12). This gives $E(V^2)_{\text{NOISE}}$ as

$$\frac{1}{4} \int_0^\infty e^{-\beta|s|} \{ \cos(\omega_0 + \delta)s + \varphi \} ds \\ \times \int_0^\infty e^{-\beta|v|} \cos\{(\omega_0 + \delta)v + \varphi\} \cos\{\omega_0(s - v)\} \\ \times \left[S_1^2 \sigma_2^2 e^{-\alpha_2|s-v|} + S_2^2 \sigma_1^2 e^{-\alpha_1|s-v|} + 2\sigma_1^2 \sigma_2^2 e^{-(\alpha_1 + \alpha_2)|s-v|} \right] dv \quad (15)$$

In order to evaluate this expression we shall first consider the second integral above which can be written as

$$\frac{1}{2} \int_0^\infty e^{-\beta|v|} \left[S_1^2 \sigma_2^2 e^{-\alpha_2|s-v|} + S_2^2 \sigma_1^2 e^{-\alpha_1|s-v|} + 2\sigma_1^2 \sigma_2^2 e^{-(\alpha_1 + \alpha_2)|s-v|} \right] \\ \times \left[\cos(\delta v + \omega_0 s + \varphi) + \cos\{(2\omega_0 + \delta)v - s\omega_0 - \varphi\} \right] dv \\ = \frac{1}{2} \int_0^\infty e^{-\beta|v|} \left\{ S_1^2 \sigma_2^2 e^{-\alpha_2|s-v|} + S_2^2 \sigma_1^2 e^{-\alpha_1|s-v|} + 2\sigma_1^2 \sigma_2^2 e^{-(\alpha_1 + \alpha_2)|s-v|} \right\} \\ \times \left[\cos v\delta \cos(s\omega_0 + \varphi) - \sin v\delta \sin(s\omega_0 + \varphi) \right. \\ \left. + \cos\{(2\omega_0 + \delta)v\} \cos(s\omega_0 - \varphi) + \sin\{(2\omega_0 + \delta)v\} \sin(s\omega_0 - \varphi) \right] dv \quad (16)$$

$$\text{Now } \int_0^\infty dv = \int_0^s dv + \int_s^\infty dv$$

and $|s - v|$ in the range $(0, s)$ is $(s - v)$

and in the range (s, ∞) is $(v - s)$

so that (16) becomes

$$\frac{1}{2} \int_0^s e^{-\beta v} \left\{ (S_1^2 \sigma_2^2 e^{-\alpha_2(s-v)} + S_2^2 \sigma_1^2 e^{-\alpha_1(s-v)} + 2\sigma_1^2 \sigma_2^2 e^{-(\alpha_1 + \alpha_2)(s-v)}) \right\} Y dv \\ + \frac{1}{2} \int_s^\infty e^{-\beta v} \left\{ (S_1^2 \sigma_2^2 e^{-\alpha_2(v-s)} + S_2^2 \sigma_1^2 e^{-\alpha_1(v-s)} + 2\sigma_1^2 \sigma_2^2 e^{-(\alpha_1 + \alpha_2)(v-s)}) \right\} Y dv \quad (17)$$

where Y is the expression in square brackets in (16). Now the second and third terms of (17) are similar to the first except for the replacement of α_2 by α_1 and $(\alpha_1 + \alpha_2)$ respectively so that we need only evaluate the general form of the integral in α and replace α by α_1 , α_2 and $(\alpha_1 + \alpha_2)$ to obtain the final expression that we need.

Let us therefore consider

$$Z(x) = \int_0^s e^{-\beta v} e^{-\alpha(s-v)} G dv + \int_s^x e^{-\beta v} e^{-\alpha(v-s)} G dv$$

$$\begin{aligned} \text{where } G = & \cos(s\omega_0 + \varphi) \cos \delta v - \sin(s\omega_0 + \varphi) \sin \delta v \\ & + \cos\{(2\omega_0 + \delta)v\} \cos(s\omega_0 - \varphi) \\ & + \sin\{(2\omega_0 + \delta)v\} \sin(s\omega_0 - \varphi) \end{aligned} \tag{18}$$

If we now make use of the integrals

$$\left. \begin{aligned} \int_0^m e^{-ax} \cos bx dx &= \frac{1}{a^2 + b^2} \{a + e^{-am} (b \sin bm - a \cos bm)\} \\ \int_0^m e^{-ax} \sin bx dx &= \frac{1}{a^2 + b^2} \{b - e^{-am} (b \cos bm + a \sin bm)\} \\ \int_m^x e^{-ax} \cos bx dx &= \frac{1}{a^2 + b^2} \{e^{-am} (a \cos bm - b \sin bm)\} \\ \int_m^x e^{-ax} \sin bx dx &= \frac{1}{a^2 + b^2} \{e^{-am} (b \cos bm + a \sin bm)\} \end{aligned} \right\} \tag{19}$$

the expression (18), after suitable reduction, becomes

$$\begin{aligned} Z(x) = e^{-\alpha s} & \left[\frac{1}{A} \{(\beta - \alpha) \cos(\omega_0 s + \varphi) - \delta \sin(\omega_0 s + \varphi)\} \right. \\ & \left. + \frac{1}{C} \{(\beta - \alpha) \cos(\omega_0 s - \varphi) + (2\omega_0 + \delta) \sin(\omega_0 s - \varphi)\} \right] \\ & + e^{-\beta s} \left[\{(\beta + \alpha) \left(\frac{1}{B} + \frac{1}{D}\right) - (\beta - \alpha) \left(\frac{1}{A} + \frac{1}{C}\right)\} \cos\{(\omega_0 + \delta)s + \varphi\} \right. \\ & \left. + \left\{ \delta \left(\frac{1}{A} - \frac{1}{B}\right) + (2\omega_0 + \delta) \left(\frac{1}{C} - \frac{1}{D}\right) \right\} \sin\{(\omega_0 + \delta)s + \varphi\} \right] \end{aligned} \tag{20}$$

$$\begin{aligned} \text{where } & \left. \begin{aligned} A &= (\beta - \alpha)^2 + \delta^2 \\ B &= (\beta + \alpha)^2 + \delta^2 \\ C &= (\beta - \alpha)^2 + (2\omega_0 + \delta)^2 \\ D &= (\beta + \alpha)^2 + (2\omega_0 + \delta)^2 \end{aligned} \right\} \tag{21} \end{aligned}$$

Thus the contribution of this term to the variance of the output noise becomes

$$\sigma_2^2 S_1^2 P(x) = \frac{1}{8} \sigma_2^2 S_1^2 \int_0^x e^{-\beta s} \cos\{(\omega_0 + \delta)s + \varphi\} Z(x) ds \text{ from (15), (17)}$$

and (20) from which we finally obtain

$$\begin{aligned}
 2 P(\alpha) = & \frac{(B+D)(\beta+\alpha)}{\beta BD} \\
 & + \cos 2\varphi \left[\left\{ \beta^2 - \alpha^2 - \delta(2\omega_0 + \delta) \right\} \left\{ \frac{1}{AD} + \frac{1}{BC} - \frac{\alpha\beta}{\beta^2 + (\omega_0 + \delta)^2} \left(\frac{1}{AB} + \frac{1}{CD} \right) \right\} \right. \\
 & \quad \left. + \frac{2\alpha\beta}{(\beta^2 + (\omega_0 + \delta)^2)} \left\{ \frac{\delta^2}{AB} + \frac{(2\omega_0 + \delta)^2}{CD} \right\} \right] \\
 & + \sin 2\varphi \left[\frac{\alpha(\omega_0 + \delta)}{\beta^2 + (\omega_0 + \delta)^2} \left\{ \beta^2 - \alpha^2 - \delta(2\omega_0 + \delta) \right\} \left\{ \frac{1}{AB} + \frac{1}{CD} \right\} \right. \\
 & \quad + 2\alpha \left\{ \frac{\delta}{AB} + \frac{(2\omega_0 + \delta)}{CD} \right\} - \frac{2\alpha(\omega_0 + \delta)}{\beta^2 + (\omega_0 + \delta)^2} \left\{ \frac{\delta^2}{AB} + \frac{(2\omega_0 + \delta)^2}{CD} \right\} \\
 & \quad \left. - \frac{2}{AD} \{ (\omega_0 + \delta)\beta - \omega_0\alpha \} - \frac{2}{BC} \{ (\omega_0 + \delta)\beta + \omega_0\alpha \} \right] \quad (22)
 \end{aligned}$$

Thus

$$E(V^2)_{\text{NOISE}} = \frac{1}{8} \{ \sigma_2^2 S_1^2 P(\alpha_2) + \sigma_1^2 S_2^2 P(\alpha_1) + 2\sigma_1^2 \sigma_2^2 P(\alpha_1 + \alpha_2) \} \quad (23)$$

Where $P(\alpha)$ is given by equation (22).

But the signal output is given by (13) and (14) as

$$\begin{aligned}
 & \frac{S_1 S_2}{2} \left[\cos(\omega_0 u) \int_0^\infty e^{-\beta|s|} \cos(\omega_0 s) \cos\{(\omega_0 + \delta)s + \varphi\} ds \right. \\
 & \quad \left. + \sin(\omega_0 u) \int_0^\infty e^{-\beta|s|} \sin(\omega_0 s) \cos\{(\omega_0 + \delta)s + \varphi\} ds \right] \\
 = & \frac{S_1 S_2}{4} \left\{ \cos(\omega_0 u) \left[\beta \cos \varphi \left(\frac{1}{\beta^2 + \delta^2} + \frac{1}{\beta^2 + (2\omega_0 + \delta)^2} \right) \right. \right. \\
 & \quad \left. \left. - \sin \varphi \left(\frac{\delta}{\beta^2 + \delta^2} + \frac{2\omega_0 + \delta}{\beta^2 + (2\omega_0 + \delta)^2} \right) \right] \right. \\
 & \quad \left. - \sin(\omega_0 u) \left[\cos \varphi \left(\frac{2\omega_0 + \delta}{\beta^2 + (2\omega_0 + \delta)^2} - \frac{\delta}{\beta^2 + \delta^2} \right) \right. \right. \\
 & \quad \left. \left. + \beta \sin \varphi \left(\frac{1}{\beta^2 + (2\omega_0 + \delta)^2} - \frac{1}{\beta^2 + \delta^2} \right) \right] \right\}
 \end{aligned}$$

so that its amplitude is

$$\frac{S_1 S_2}{4} \left\{ \left[\beta \cos \varphi \left(\frac{1}{\beta^2 + \delta^2} + \frac{1}{\beta^2 + (2\omega_0 + \delta)^2} \right) - \sin \varphi \left(\frac{\delta}{\beta^2 + \delta^2} + \frac{2\omega_0 + \delta}{\beta^2 + (2\omega_0 + \delta)^2} \right) \right] \right\}$$

$$\begin{aligned}
 & + \left[\cos \varphi \left(\frac{2\omega_0 + \delta}{\beta^2 + (2\omega_0 + \delta)^2} - \frac{\delta}{\beta^2 + \delta^2} \right) + \beta \sin \varphi \left(\frac{1}{\beta^2 + (2\omega_0 + \delta)^2} - \frac{1}{\beta^2 + \delta^2} \right) \right]^2 \Bigg\}^{\frac{1}{2}} \\
 & = \frac{S_1 S_2}{4} \left\{ \frac{1}{\beta^2 + \delta^2} + \frac{1}{\beta^2 + (2\omega_0 + \delta)^2} + \frac{2 \cos 2\varphi \{ \beta^2 - \delta (2\omega_0 + \delta) \}}{(\beta^2 + \delta^2) \{ \beta^2 + (2\omega_0 + \delta)^2 \}} \right. \\
 & \quad \left. - \frac{4\beta (\omega_0 + \delta) \sin 2\varphi}{(\beta^2 + \delta^2) \{ \beta^2 + (2\omega_0 + \delta)^2 \}} \right\}^{\frac{1}{2}} \tag{24}
 \end{aligned}$$

which is seen to be equal to

$$\frac{S_1 S_2}{4} \sqrt{2 P(0)}$$

by putting $\alpha = 0$ in equation (22)

thus the signal/noise ratio is given by

$$\frac{S_1 S_2}{\sigma_1 \sigma_2} \left\{ \frac{S_2^2}{\sigma_2^2} P(\alpha_1) + \frac{S_1^2}{\sigma_1^2} P(\alpha_2) + 2P(\alpha_1 + \alpha_2) \right\}^{\frac{1}{2}} \tag{25}$$

here we note $\frac{S_1}{\sigma_1}, \frac{S_2}{\sigma_2}$ are the signal/noise ratios of the input voltages.

Approximate Solutions

The result obtained for the case of a single tuned circuit (equation (24)) is still general in its application and complicated in its evaluation and we shall, in this section, seek to simplify the result by means of further assumptions. We shall classify the results which are obtained by making these assumptions, according to the following scheme:

- I. ω_0 large by comparison with $\alpha_1, \alpha_2, \beta$.
- II. $\omega_0 \doteq \alpha_1, \alpha_2$
- III. $\omega_0 + \delta = 0$. (The case of an R.C. circuit).

These three cases will be subdivided into:

- (a) α_1, α_2 large by comparison with β, δ .
- (b) $\beta = \alpha_1 = \alpha_2 = \alpha$.

and a further subdivision

- (i) Circuit in tune, i.e. $\delta = 0$.
- (ii) Circuit tuned to edge of bandwidth of beatnote, i.e. $\delta = \beta$.

We shall derive the requisite expressions dependent upon the above assumptions and then summarize the position by comparison at the end.

Case I ($\omega_0 \gg \alpha_1, \alpha_2, \beta$).

The expression for $P(\alpha)$ reduces to

$$P(\alpha) = \frac{1}{2} \left\{ \frac{\alpha + \beta}{\beta \{(\beta + \alpha)^2 + \delta^2\}} \right\} + \text{terms of order } \frac{1}{\omega_0}$$

$$\text{and } P(0) = \frac{1}{2} \left\{ \frac{1}{\beta^2 + \delta^2} \right\} + \text{terms of order } \frac{1}{\omega_0} \quad (26)$$

hence the signal/noise ratio is given by

$$\frac{S_1 S_2}{\sigma_1 \sigma_2} \left\{ \frac{\beta}{(\beta^2 + \delta^2)} \left\{ \frac{S_2^2}{\sigma_2^2} \left(\frac{\beta + \alpha_1}{(\beta + \alpha_1)^2 + \delta^2} \right) + \frac{S_1^2}{\sigma_1^2} \left(\frac{\beta + \alpha_2}{(\beta + \alpha_2)^2 + \delta^2} \right) + \frac{2(\beta + \alpha_1 + \alpha_2)}{(\beta + \alpha_1 + \alpha_2)^2 + \delta^2} \right\} \right\} \quad (27)$$

If we then proceed to the subdivisions we shall get

$$\beta \ll \alpha, \text{ Ia : Signal/noise} = \frac{S_1 S_2}{\sigma_1 \sigma_2} \left\{ \frac{\beta}{(\delta^2 + \beta^2)} \left\{ \frac{1}{\alpha_1} \frac{S_2^2}{\sigma_2^2} + \frac{1}{\alpha_2} \frac{S_1^2}{\sigma_1^2} + \frac{2}{\alpha_1 + \alpha_2} \right\} \right\}^{\frac{1}{2}} \quad (28)$$

$$\beta = \alpha, \text{ Ib : Signal/noise} = \frac{S_1 S_2}{\sigma_1 \sigma_2} \left\{ \frac{\alpha}{(\alpha^2 + \delta^2)} \left\{ \frac{2\alpha}{4\alpha^2 + \delta^2} \left(\frac{S_1^2}{\sigma_1^2} + \frac{S_2^2}{\sigma_2^2} \right) + \frac{6\alpha}{9\alpha^2 + \delta^2} \right\} \right\}^{\frac{1}{2}} \quad (29)$$

and hence

$$\delta = 0, \text{ Ia(i): Signal/noise} = \frac{S_1 S_2}{\sigma_1 \sigma_2} \left\{ \frac{1}{\beta} \left\{ \frac{S_2^2}{\alpha_1 \sigma_2^2} + \frac{S_1^2}{\alpha_2 \sigma_1^2} + \frac{2}{\alpha_1 + \alpha_2} \right\} \right\}^{\frac{1}{2}} \quad (30)$$

$$\delta = \beta, \text{ Ia(ii): Signal/noise} = \frac{S_1 S_2}{\sigma_1 \sigma_2} \left\{ \frac{1}{2\beta} \left\{ \frac{S_2^2}{\alpha_1 \sigma_2^2} + \frac{S_1^2}{\alpha_2 \sigma_1^2} + \frac{2}{\alpha_1 + \alpha_2} \right\} \right\}^{\frac{1}{2}} \quad (31)$$

$$\delta = 0, \text{ Ib(i) Signal/Noise} = \frac{S_1 S_2}{\sigma_1 \sigma_2} \left\{ \frac{1}{2} \left(\frac{S_1^2}{\sigma_1^2} + \frac{S_2^2}{\sigma_2^2} \right) + \frac{2}{3} \right\}^{\frac{1}{2}} \quad (32)$$

$$\delta = \beta, \text{ Ib(ii) Signal/Noise} = \frac{S_1 S_2}{\sigma_1 \sigma_2} \left\{ \frac{1}{2} \left\{ \frac{2}{5} \left(\frac{S_1^2}{\sigma_1^2} + \frac{S_2^2}{\sigma_2^2} \right) + \frac{3}{5} \right\} \right\}^{\frac{1}{2}} \quad (33)$$

From (30) and (31) we see that the effect of being out of tune is to reduce the signal/noise ratio by $1/\sqrt{2}$ or 3 dB in the case where $\beta \ll \alpha$.

In the case of $\beta = \alpha$ we see from (32) and (33) that the effect of being out of tune is to reduce the signal/noise ratio by a factor

$$\frac{\left\{ 8 \left(\frac{S_1^2}{\sigma_1^2} + \frac{S_2^2}{\sigma_2^2} + \frac{3}{2} \right) \right\}^{\frac{1}{2}}}{\left\{ 5 \left(\frac{S_1^2}{\sigma_1^2} + \frac{S_2^2}{\sigma_2^2} + \frac{4}{3} \right) \right\}^{\frac{1}{2}}} \quad (34)$$

which varies between $\sqrt{\frac{8}{5}}$ when $\frac{S_1}{\sigma_1}$ and/or $\frac{S_2}{\sigma_2}$ are large and $\sqrt{\frac{9}{5}}$ when $\frac{S_1}{\sigma_1}$, $\frac{S_2}{\sigma_2}$ are small, i.e. a loss of 2 dB and 2.6 dB respectively.

Let us now compare Ia with Ib; to make things equivalent we take $\alpha_1 = \alpha_2 = \alpha$ in Ia as has been done in Ib and since we know the effect of mistuning in each case we shall consider only the case when they are both in tune. From (30) and (32) we get for the ratio of the two signal/noise

$$\left\{ \frac{\alpha \left(\frac{S_2^2}{\sigma_2^2} + \frac{S_1^2}{\sigma_1^2} + \frac{4}{3} \right)}{2\beta \left(\frac{S_2^2}{\sigma_2^2} + \frac{S_1^2}{\sigma_1^2} + 1 \right)} \right\}^{\frac{1}{2}} = \sqrt{\frac{\alpha}{2\beta}} \quad (35)$$

since the second factor only varies between 1 and 1.33, so that the gain in having a narrow bandwidth for the beatnote is $10 \log_{10} \left(\frac{\alpha}{2\beta} \right)$ dB.

Case II ($\omega_0 = \alpha_1, \alpha_2, \beta$)

For subdivision IIa, when $\alpha_1, \alpha_2 \gg \beta$ the expression for $P(\alpha)$ becomes

$$\frac{1}{2} \left\{ \frac{\alpha}{\beta} \left(\frac{1}{\alpha^2} + \frac{1}{\alpha^2 + 4\omega_0^2} \right) \right\} \quad (36)$$

and is the same for $\delta = 0$ and $\delta = \beta$ for since $\beta \ll \alpha$ and $0 \ll \delta \ll \beta$ then *à fortiori* $\delta \ll \alpha$.

The expression for $P(0)$ however becomes

$$\begin{aligned} & \frac{1}{2} \left\{ \frac{1}{\beta^2} \right\} \text{ for IIa(i)} \\ \text{and } & \frac{1}{2} \left\{ \frac{1}{2\beta^2} \right\} \text{ for IIa(ii)} \end{aligned} \quad (37)$$

so that we have that the effect of being out of tune is to leave the noise output unaffected and to reduce the signal output by $1/\sqrt{2}$, i.e. the signal/noise ratio is reduced by 3 dB.

In the case of subdivision IIb, i.e. when $\alpha = \beta$, the expressions for $P(\alpha)$ do not simplify very much so we make a further assumption that $\omega_0 = \alpha$. We then obtain for IIb(i), when $\delta = 0 = \varphi$, that the signal/noise ratio is given by

$$\frac{S_1 S_2}{\sigma_1 \sigma_2} \left\{ \frac{8}{5 \left(\frac{S_1^2}{\sigma_1^2} + \frac{S_2^2}{\sigma_2^2} + \frac{20}{13} \right)} \right\}^{\frac{1}{2}} \quad (38)$$

and for IIb(ii) when $\delta = \beta$ we get the signal noise ratio to be

$$\frac{S_1 S_2}{\sigma_1 \sigma_2} \left\{ \frac{195 (3 - \cos 2\varphi - 2 \sin 2\varphi)}{2 \left\{ 30 \left(\frac{S_1^2}{\sigma_1^2} + \frac{S_2^2}{\sigma_2^2} \right) (9 - \cos 2\varphi - 5 \sin 2\varphi) + 13(35 - \cos 2\varphi - 18 \sin 2\varphi) \right\}} \right\}^{\frac{1}{2}} \quad (39)$$

hence the effect of being out of tune is to reduce the signal/noise ratio by the factor

$$\left\{ \frac{16 \left\{ 30(9 - \cos 2\varphi - 5 \sin 2\varphi) \left(\frac{S_1^2}{\sigma_1^2} + \frac{S_2^2}{\sigma_2^2} \right) + 13(35 - \cos 2\varphi - 18 \sin 2\varphi) \right\}}{75 \left\{ 13 \left(\frac{S_1^2}{\sigma_1^2} + \frac{S_2^2}{\sigma_2^2} \right) + 20 \right\} \left\{ 3 - \cos 2\varphi - 2 \sin 2\varphi \right\}} \right\}^{\frac{1}{2}} \quad (40)$$

as obtained from (38) and (39).

The behaviour of this expression throughout the range of φ is depicted in Fig. 1. The upper boundary is the case when $\frac{S_1}{\sigma_1}, \frac{S_2}{\sigma_2}$ are very small and

the lower boundary the case when $\frac{S_1}{\sigma_1}$ or $\frac{S_2}{\sigma_2}$ or both are large. From Fig.

it is seen that the effect of tuning is least when $\varphi = \frac{\pi}{2}$ and greatest when

$\varphi = \frac{\pi}{6}$ and represents a loss of 5 dB in the worst case and a loss of 1 dB in the best.

The comparison between the Cases IIa(i), ($\alpha \gg \beta$) and IIb(i) ($\alpha = \beta$) gives from (36), (37) and (38) a reduction factor of

$$\left\{ \frac{25\alpha \left(\frac{S_1^2}{\sigma_1^2} + \frac{S_2^2}{\sigma_2^2} + \frac{20}{13} \right)}{12\beta \left(4 \left(\frac{S_1^2}{\sigma_1^2} + \frac{S_2^2}{\sigma_2^2} \right) + 5 \right)} \right\}^{\frac{1}{2}} \quad (41)$$

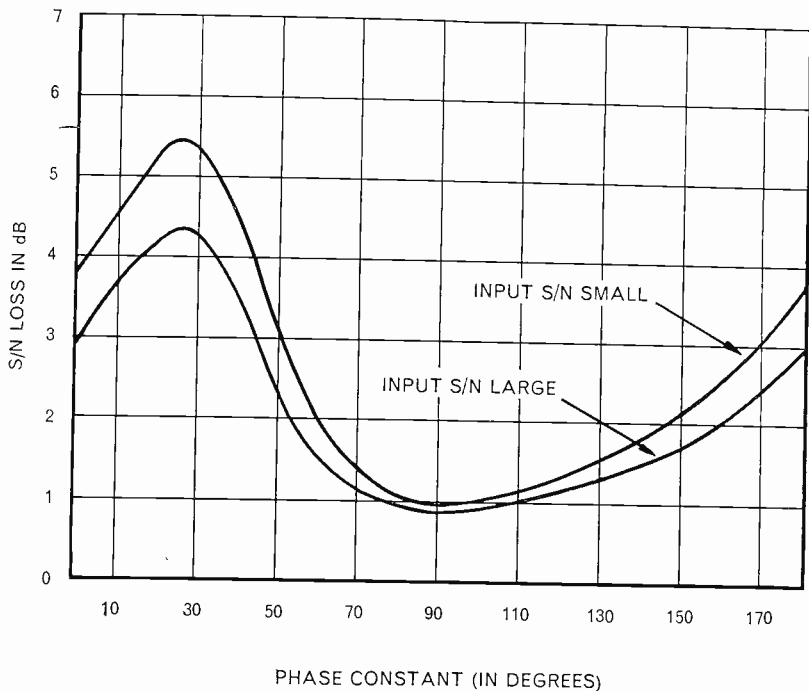


Fig. 1. Effects of Mistuning

which varies between $\sqrt{\frac{25\alpha}{48\beta}}$, when $\frac{S_1}{\sigma_1}$ or $\frac{S_2}{\sigma_2}$ or both are large, and $\sqrt{\frac{25}{39} \frac{\alpha}{\beta}}$ when $\frac{S_1}{\sigma_1}, \frac{S_2}{\sigma_2}$ are small.

Case III (An R.C. circuit when $\omega_0 + \delta = 0$ and $\varphi = 0$)

In this case $P(\alpha)$ reduces to

$$\frac{1}{2} \left\{ \frac{4(\alpha + \beta)}{\beta [(\alpha + \beta)^2 + \delta^2]} \right\}$$

and $P(0)$ to $\frac{1}{2} \left\{ \frac{4}{\beta^2 + \delta^2} \right\}$ giving as the signal/noise ratio the expression

$$\frac{S_2}{\sigma_2} \left\{ \frac{\beta}{(\beta^2 + \delta^2) \left\{ \frac{S_2^2}{\sigma_2^2} \left(\frac{\beta + \alpha_1}{(\beta + \alpha_1)^2 + \delta^2} \right) + \frac{S_1^2}{\sigma_1^2} \left(\frac{\beta + \alpha_2}{(\beta + \alpha_2)^2 + \delta^2} \right) + \frac{2(\beta + \alpha_1 + \alpha_2)}{(\beta + \alpha_1 + \alpha_2)^2 + \delta^2} \right\}} \right\}^{\frac{1}{2}} \quad (42)$$

which is seen to be the same expression as that of Case I by equation (27), so that these two cases are identical and any results obtained in the two cases must be the same.

From these results we see that in each of the three Cases I, II, III, the best results are obtained when the circuit is in tune and the beatnote bandwidth is small in comparison with the input bandwidths. Since Cases I and III are identical, if we compare the signal/noise ratios of IIa(i) and Ia(i) we get an overall picture of the losses incurred in the different cases.

The signal/noise ratio for Case Ia(i) is

$$\frac{S_1 S_2}{\sigma_1 \sigma_2} \left\{ \beta \left(\frac{S_2^2}{\sigma_2^2} \cdot \frac{1}{\alpha_1} + \frac{S_1^2}{\sigma_1^2} \cdot \frac{1}{\alpha_2} + \frac{2}{\alpha_1 + \alpha_2} \right) \right\}^{-\frac{1}{2}} \tag{43}$$

and for the Case IIa(i) it is

$$\frac{S_1 S_2}{\sigma_1 \sigma_2} \left\{ \beta \left[\frac{S_2^2}{\sigma_2^2} \frac{1}{\alpha_1} \left(1 + \frac{\alpha_1^2}{\alpha_1^2 + 4\omega_0^2} \right) + \frac{S_1^2}{\sigma_1^2} \frac{1}{\alpha_2} \left(1 + \frac{\alpha_2^2}{\alpha_2^2 + 4\omega_0^2} \right) + \frac{2}{(\alpha_1 + \alpha_2)} \left(1 + \frac{(\alpha_1 + \alpha_2)^2}{(\alpha_1 + \alpha_2)^2 + 4\omega_0^2} \right) \right] \right\}^{-\frac{1}{2}} \tag{44}$$

and the ratio of these two terms, if $\alpha_1 = \alpha_2$, is

$$\left\{ \frac{\left(\frac{S_1^2}{\sigma_1^2} + \frac{S_2^2}{\sigma_2^2} \right) \left(1 + \frac{\alpha^2}{\alpha^2 + 4\omega_0^2} \right) + 1 + \frac{\alpha^2}{\alpha^2 + \omega_0^2}}{\frac{S_1^2}{\sigma_1^2} + \frac{S_2^2}{\sigma_2^2} + 1} \right\}^{\frac{1}{2}}$$

which varies between $\sqrt{1 + \frac{\alpha^2}{\alpha^2 + 4\omega_0^2}}$ and $\sqrt{1 + \frac{\alpha^2}{\alpha^2 + \omega_0^2}}$ if

$\frac{S_1}{\sigma_1}, \frac{S_2}{\sigma_2}$ are very large and very small respectively, and this becomes a range of .8dB to 1.5dB in the case of $\omega_0 = \alpha$. This means that the optimum result is obtained for the case of a circuit in tune with small beatnote bandwidth in comparison with the input bandwidths and the midband frequency of the output either small or large by comparison with the input bandwidths.

Summary of Results

From the preceding section we have seen how variations in the input/output bandwidth ratio, the amount of mistuning and the size of the beatnote mid-band frequency have affected the signal/noise ratio of the beatnote. Since we can measure these effects relative to each other we can choose one of them as the norm to be examined for the total effect of

mixing two noisy signals and describe the other effects as corrections to be applied to that norm. We have chosen the case of Ia(i) (which as we have seen is equivalent to IIIa(i)) where $\omega_0 \gg \beta$, $\alpha \ll \beta$, $\delta = 0$ as the norm since this gives the optimum results.

From equation (43), by putting $\alpha_1 = \alpha$ and $\alpha_2 = q\alpha_1$ we get the signal/noise ratio of the norm to be:

$$\frac{S_1}{\sigma_1} \sqrt{\frac{\alpha}{\beta}} \left(\frac{S_2/\sigma_2}{\sqrt{S_2^2/\sigma_2^2 + S_1^2/q\sigma_1^2 + 2/q + 1}} \right) = \frac{S_1}{\sigma_1} \sqrt{\frac{\alpha}{\beta}} M \tag{45}$$

We note that the above expression, when $\sigma_2 = 0$ giving $M = 1$, is the well known expression obtained when mixing a noisy signal with a clean signal, hence M gives a measure of the effect obtained when the second signal is also noisy. We give in Table I, the corrections that have to be applied to M for all the other cases considered in the previous section for the case of $q = 1$.

TABLE I
Corrections (in dB) to be applied to the norm.

$\delta = 0$		$\delta = \beta$			
	$\beta \ll \alpha$	$\beta = \alpha$	$\beta \ll \alpha$	$\beta = \alpha$	
Case I $\omega_0 \gg \alpha$	0dB (Norm)	3dB	-3dB	1dB 0.4dB	U L
Case II $\omega_0 = \alpha_0$	-1dB -1.5dB	2dB 0.5dB	-4dB -4.5dB	(2-B)dB (0.5-B)dB	U L
Case III $\omega_0 + \delta = 0$	0dB (Norm)	3dB	-3dB	1dB 0.4dB	U L

where $B =$ a loss varying between 1dB and 5dB and is dependent upon the phase constant φ (see Fig. 1).

U } = Range bracket determined by signal/noise of input being very
L } large or very small respectively.

$\alpha/\pi, \beta/\pi$ are the input and output bandwidths taken between the 3dB points.

$\delta =$ the divergence of the natural oscillation of the filter from the beat-note frequency

$\omega_0 =$ the beatnote frequency in rad/sec.

The reason for the apparent gain in the case of $\beta = \alpha$ over the case of $\beta \ll \alpha$ can be seen most easily in the case of one noisy signal and one clean signal (i.e. $\sigma_2 = 0$) where the noisy signal in effect passes through two single-tuned circuits with the same bandwidth. This has the effect of reducing the effective noise bandwidth by $\frac{1}{2}$ or gives a gain of 3dB over one single-tuned circuit. In the case where $\omega_0 \cong \alpha, \beta$ the lack of symmetry due to the beatnote bandwidth being equal to the mid-frequency increases the effective noise bandwidth.

As an illustration of how to use this table let us suppose we wish to find the signal/noise ratios of the output voltages for the cases of $\omega_0 \gg \alpha, \beta = \alpha, \delta = 0$ and $\omega_0 + \delta = 0, \beta \ll \alpha, \delta = \beta$ (i.e. Ib(i) and IIIa (ii)). We are given the signal/noise ratio for the norm (see equation 45) so for the first example we add on 3dB, whilst for the second we subtract 3dB. Hence we see that, in the first example, although there is an increase of signal/noise of 3dB over the norm there is also a loss equal to bandwidth ratio α/β exacted by increasing β from being $\ll \alpha$ to equality with α .

Finally we give a few examples which show how the effect of mixing two noisy signals compares with the case when one input has no noise (e.g. a local oscillator). To judge this effect we shall use the norm of Table I and any other cases can, of course, be dealt with by reference to that Table. Our calculations therefore are based upon (43), which in the case of one input signal being noiseless ($\sigma_2 = 0$) gives a signal/noise ratio of

$$S_1/\sigma_1 \sqrt{\alpha/\beta} \tag{46}$$

For our calculations we shall take $\alpha/\beta = 500$ (i.e. 27dB) and

$$S_1/\sigma_1 = \sqrt{\frac{1}{500}}$$

so that (46) gives a beatnote signal/noise ratio of unity. If we now admit noise on to the second signal we shall get a decrease of signal/noise as shown in Table II.

TABLE II
Case of $\alpha_1 = \alpha_2$

S_2/σ_2	∞ dB	0dB	-3dB	-10dB	-27dB
loss	0dB	-3dB	-5.2dB	-10.4dB	-27dB

One way that we can repair the loss of signal/noise is by decreasing the bandwidth of one of the input signals. As an example of this we take the case of $\alpha_2 = 500\alpha_1$, then S_2/σ_2 will increase by $\sqrt{500}$. The effect on the results of Table II are given in Table III.

TABLE III

$$\alpha_2 = 500\alpha_1$$

S_2/σ_2	∞ dB	27dB	24dB	17dB	0dB
loss	0dB	0dB	0dB	0dB	-0.01dB

Conclusion

This article has had as its object the investigation into the effect of mixing two signals when each has noise present with it. The general analytical expression was obtained but in order to proceed from this it was necessary to deal with less general cases and even in these cases the resultant expressions were very complicated and progress could only be made by making various assumptions regarding the bandwidths of the input and output signals and mid-band frequency of the output. The actual cases chosen were those which were most likely to occur in practice. These restrictions naturally limited the scope of this article but a full investigation would be a formidable task. The forms of the expressions resulting from the choice of the impulse response and auto-correlations in most cases would be intractable mathematically and any attempt at a solution would involve the use of electronic computers.

Acknowledgements

The author would like to acknowledge the help and guidance given him in the preparation of this article by Mr. P. S. Brandon.

BOOK REVIEW

UHF LINE TECHNIQUES by C. S. Gledhill

Edward Arnold (Publishers) Ltd. Price 12s. 6d.

This should be a very useful collection of formulae and methods for using transmission lines to perform multiple functions in communication circuits.

Unfortunately, the author seems to rely too much on other publications, even going so far as to introduce symbols without first defining them (e.g. in the equation which forms the basis of Smith's Chart construction). The Smith's Chart is very properly used as the basis of all manipulations with

impedances, but it is not very clearly introduced to a beginner.

Otherwise, this little booklet contains many useful carefully chosen examples and is copiously illustrated: stub matching (single and multiple), the impedance slope and line length compensation, transformer techniques, are all adequately covered. The essential theoretical unity of circuits with lumped and with distributed parameters is brought to the fore by the competent use of Smith's Chart for the latter.

A NOTE ON DIFFRACTION ROUND A SPHERE OR CYLINDER

By G. MILLINGTON, M.A., B.Sc., M.I.E.E.

The problem of the diffraction of radio waves round a sphere or cylinder is treated as a generalization of the known solution for propagation over a smooth spherical earth. An approximate simplified method of solving the eigen-value equation is given for vertically and horizontally polarized waves that is accurate enough for practical purposes and curves are presented for the first term of the diffraction formula. The results are applied to propagation over rounded hilltops where the attenuation is effectively exponential with distance and some indication is given of the transition from this treatment to the use of Fresnel theory for an equivalent knife-edge as the receiver is moved out of the shadow region of the hill.

This note is based very largely on an unpublished report written by the author nearly twenty years ago which followed up some conclusions derived by Eckersley and Millington⁽¹⁾. They had shown that at least at very high frequencies the field-strength received at an elevation large compared with a height of about $50\lambda^{2/3}$ metres (λ is the wavelength in metres) from a similarly well elevated transmitter over a smooth earth could be approximately regarded as in Fig. 1. The receiver at R is well below the line of sight of the transmitter at T with respect to a sphere concentric with the earth but with a radius greater by the $50\lambda^{2/3}$ metres quoted above. Along the tangents TA and BR the propagation is effectively free space, while between A and B the attenuation is exponential and characteristic of the diffraction loss with distance in the shadow region in ground-wave propagation beyond the horizon.

This observation led to the suggestion that in propagation over a well rounded hill the diffraction loss could be estimated in terms of the attenuation round an equivalent sphere or cylinder, as indicated in Fig. 2, by a generalization of the smooth earth analysis. It is interesting to note that subsequently McPetrie and Ford⁽²⁾ made measurements over bare ridges of well defined curvature (see also the discussion on the paper by Domb and Pryce⁽³⁾) which confirmed the exponential form of the attenuation with distance, while Bremmer⁽⁴⁾ has discussed the mathematical basis of the propagation mechanism in terms of Fig. 2 as derived from the classical van der Pol and Bremmer diffraction analysis.

A considerable amount of work has now been done on the estimation of diffraction losses over hilly or mountainous terrain in which the alternative treatments in terms of Fresnel knife-edge theory and of curved earth

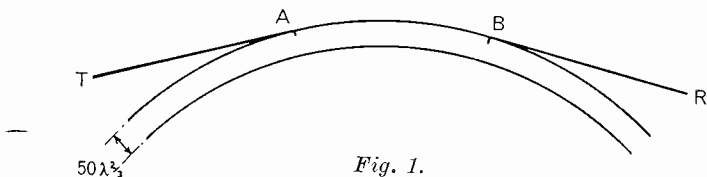


Fig. 1.

analysis have been compared, an early paper being one by Matsuo⁽⁵⁾. The main purpose of presenting the following discussion of a limited aspect of the problem at this late date is to provide a simple treatment of diffraction round a sphere or cylinder based on the method of Eckersley and Millington. In particular it gives an approximate solution of the difficult eigen-value equation involved which is found to be sufficiently accurate for practical purposes.

General Statement of the Problem

In the diffraction of radio waves round the earth we have a particular case of the more general problem of diffraction round a sphere. As far as the exponential attenuation with distance round a curved surface is concerned, the analysis is also applicable to the problem of diffraction round a cylinder, for if we consider an infinitely long cylinder and an infinite line source parallel to its axis, the analysis leads to effectively the same eigen-value equation as in the case of a sphere of the same radius.

In adapting the analysis for diffraction round the earth, we have only to work out the detailed effect of replacing the radius of the earth by that of the sphere or cylinder, and this is not a difficult procedure provided that we retain the condition $x \gg 1$, where

$$x = \frac{2\pi r_0}{\lambda} \tag{1}$$

r_0 being the radius and λ the wavelength in the same units. When $\lambda = 0.5 r_0$, $x = 4\pi$, i.e. > 10 , so that we will adopt as our condition that the wavelength must be less than half the radius of the sphere or cylinder.

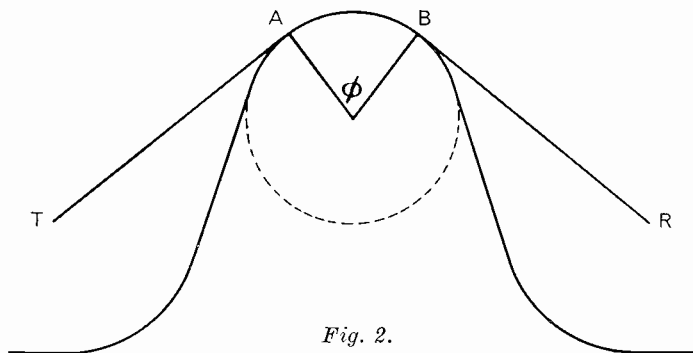


Fig. 2.

If the angle through which the wave is diffracted is φ shown in Fig. 2, corresponding to a distance d given by

$$d = r_0 \varphi \quad (2)$$

the exponential attenuation can be represented by a factor $\exp(-\alpha \varphi)$ where

$$\alpha = x^{\frac{1}{3}} |\rho| \sin\left(\frac{\pi}{3} - \omega\right) \quad (3)$$

in which $|\rho|$ and ω are the modulus and phase of a complex quantity which is the solution of the eigen-value equation.

This equation is obtained by satisfying the condition that a solution of the wave equation that represents a single outgoing wave at sufficiently large distances from the sphere or cylinder satisfies the boundary conditions for reflection at the surface, where by reason of the Stokes phenomenon the solution has the form of an outgoing and incoming pair of waves. The reflection coefficient depends upon the dielectric constant and the conductivity of the material of the sphere or cylinder which enter the eigen-value equation through a quantity η defined by

$$\eta = \frac{x^{\frac{1}{3}} \exp\left(j \frac{\pi}{6}\right)}{\zeta \sqrt{2\rho}} \quad (4)$$

Here ζ is a function of the earth constants that is different for vertically and horizontally polarized waves.

For vertical polarization

$$\zeta = \frac{\varepsilon - j 60\sigma\lambda}{\sqrt{\varepsilon - 1 - j 60\sigma\lambda}} \quad (5)$$

while for horizontal polarization

$$\zeta = \frac{1}{\sqrt{\varepsilon - 1 - j 60\sigma\lambda}} \quad (6)$$

where ε is the dielectric constant relative to that of free space while σ is the conductivity in mhos per metre when λ is measured in metres. The forms in equations (4), (5) and (6) are appropriate to the use of a positive time factor in solving the wave equation.

It will be seen that equation (4) depends upon the value of ρ , while the eigen-value equation is a complicated relation in ρ and η expressed in terms of Hankel functions of order one-third. Eckersley and Millington used the so-called tangent approximation, which they derived from Eckersley's phase-integral treatment, in the form

$$\rho = \rho_0 [1 + A \tan^{-1} \eta]^{\frac{2}{3}} \quad (7)$$

in which ρ_0 is the long wave limit as $\lambda \rightarrow \infty$ for vertical polarization,

equivalent to $\sigma = \infty$ for perfect conductivity, i.e. where ζ in equation (5) is ∞ and η in equation (4) is zero. It is given from the tangent approximation by

$$\rho_0 = \frac{1}{2} \left[3\pi \left(s + \frac{1}{4} \right) \right]^{\frac{2}{3}} \quad (8)$$

in which s can have the discrete values 0, 1, 2 etc. corresponding to the infinite number of terms of the so-called residue series for the field-strength in the diffraction region. We shall limit our consideration to distances beyond the horizon for which the first term corresponding to $s = 0$ is predominant, so that equation (8) gives

$$\rho_0 = \frac{1}{2} \left[\frac{3\pi}{4} \right]^{\frac{2}{3}} = 0.885 \quad (9)$$

The value of A in equation (7) is given by

$$A = \frac{1}{\pi \left(s + \frac{1}{4} \right)} \quad (10)$$

which for $s = 0$ gives

$$A = \frac{4}{\pi} = 1.273 \quad (11)$$

At the short wave limit when $\lambda \rightarrow 0$, $x \rightarrow \infty$ and from equation (4) $\eta \rightarrow \infty$ both for vertical and horizontal polarization. In equation (7)

$\pi^{-1}\eta \rightarrow \frac{\pi}{2}$ and ρ approaches an upper limit ρ_x given from equations (7), (9) and (10) by

$$\rho_x = \frac{1}{2} \left[\frac{9\pi}{4} \right]^{\frac{2}{3}} = 1.842 \quad (12)$$

At the long wave limit for horizontal polarization ρ also approaches ρ_x since ζ in equation (4) given by equation (6) approaches zero as $\lambda^{-\frac{1}{2}}$ whereas $x^{1/3}$ from equation (1) approaches zero as $\lambda^{-\frac{1}{2}}$.

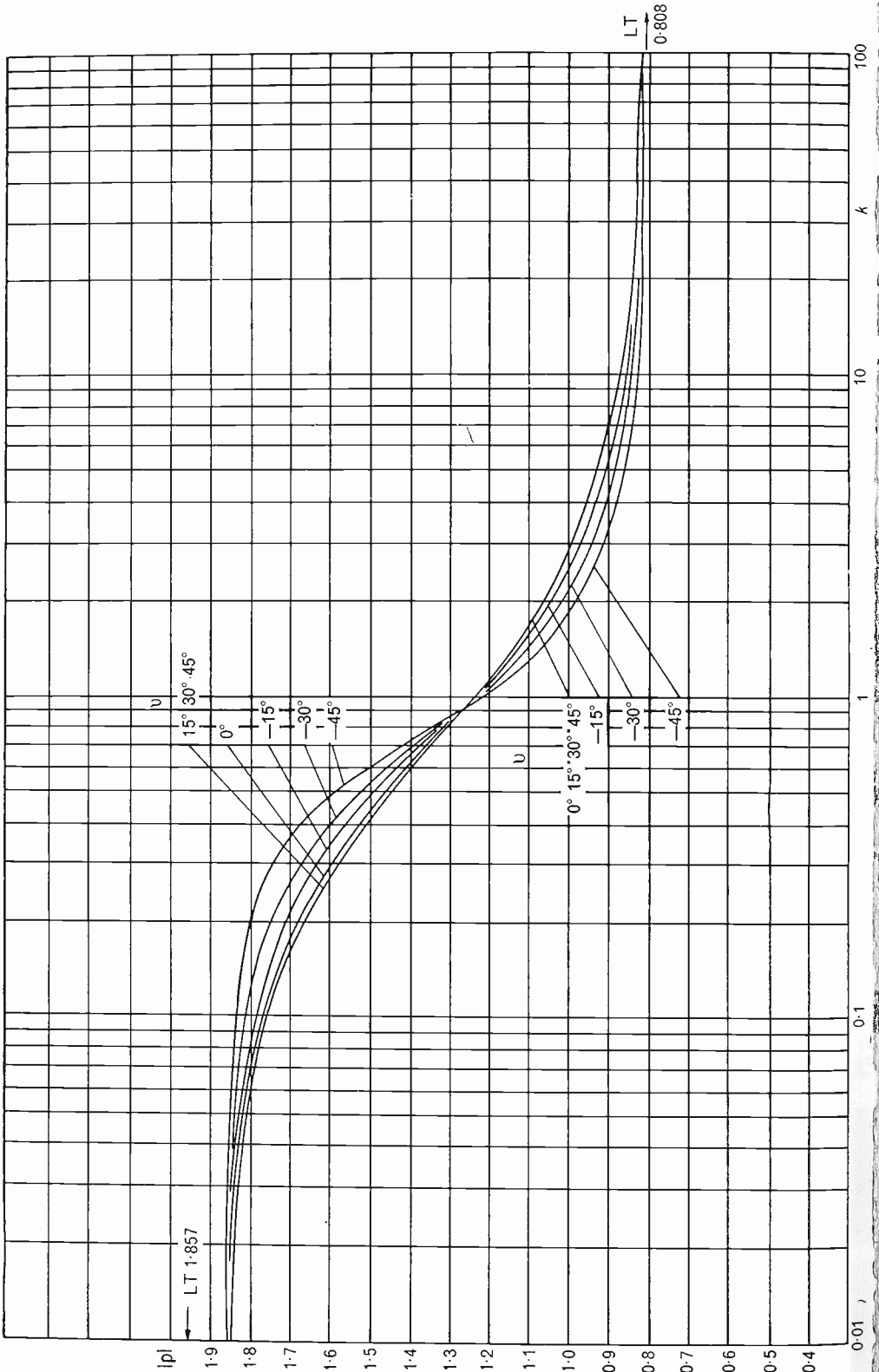
Solution of the Eigen-Value Equation

The limiting values of ρ_0 and ρ_x in equations (9) and (12) are somewhat in error and it can be shown that the true values given by using the Hankel form of the eigen-value equation are respectively

$$\rho_0 = 0.808 \quad (13)$$

$$\rho_x = 1.857 \quad (14)$$

For values between these limits ρ is complex since the quantity η in equation (4) is complex. As η also involves ρ itself, this raises great difficulties in solving the eigen-value equation. Indeed this has so far been



done with the Hankel form by using asymptotic expansions appropriate to the cases where ρ is nearer to ρ_0 and ρ_x respectively, which become inaccurate in the middle region where ρ passes through a rapid transition from values near to ρ_0 to those near to ρ_x .

Eckersley and Millington showed that the essential nature of this transition was contained in the solution of an equation of the tangent type in equation (7) and moreover that this could be solved over the whole range of ρ values by a rapidly convergent iterative process by using the known expansion into its real and imaginary parts of an inverse tangent of complex argument.

They further adopted the device of adjusting the term $\frac{1}{4}$ that occurs in equations (8) and (10) to give ρ_0 , calculated from equation (8) with $s = 0$, its true value given in equation (13) in place of the value in equation (9). This did, however, have the effect of decreasing the value of ρ_x somewhat below the value given in equation (12) and further from the true value in equation (14). Here this type of adjustment is carried further by giving ρ_0 in equation (7) its true value and choosing A to make ρ the true value of ρ_x when $\tan^{-1}\tau_1 = \frac{\pi}{2}$.

From now on, ρ_0 and ρ_x will be defined by their true values, and in terms of them the above definition of A gives

$$A = \frac{2}{\pi} \left[\left(\frac{\rho_x}{\rho_0} \right)^{\frac{3}{2}} - 1 \right] = 1.580 \quad (15)$$

This value is admittedly markedly different from the value in equation (11), but it is found that the values of ρ derived from equation (7) agree well with those obtained from the Hankel form of the equation and are amply good for the type of practical application considered in the present article.

It is useful to convert equation (7) to the form

$$\rho = \rho_0 \cdot \left[1 - B \tan^{-1} \frac{1}{\tau_1} \right]^{\frac{2}{3}} \quad (16)$$

for computation for values near to ρ_x , where B is found by putting

$\rho = \rho_0$ when $\tan^{-1} \frac{1}{\tau_1} = \frac{\pi}{2}$, so that

$$B = \frac{2}{\pi} \left[1 - \left(\frac{\rho_0}{\rho_x} \right)^{\frac{3}{2}} \right] = 0.454 \quad (17)$$

The forms of ρ in equations (7) and (16) are strictly equivalent and can be used throughout the whole range of ρ . It is a mere matter of convenience in computation to use one form rather than the other according

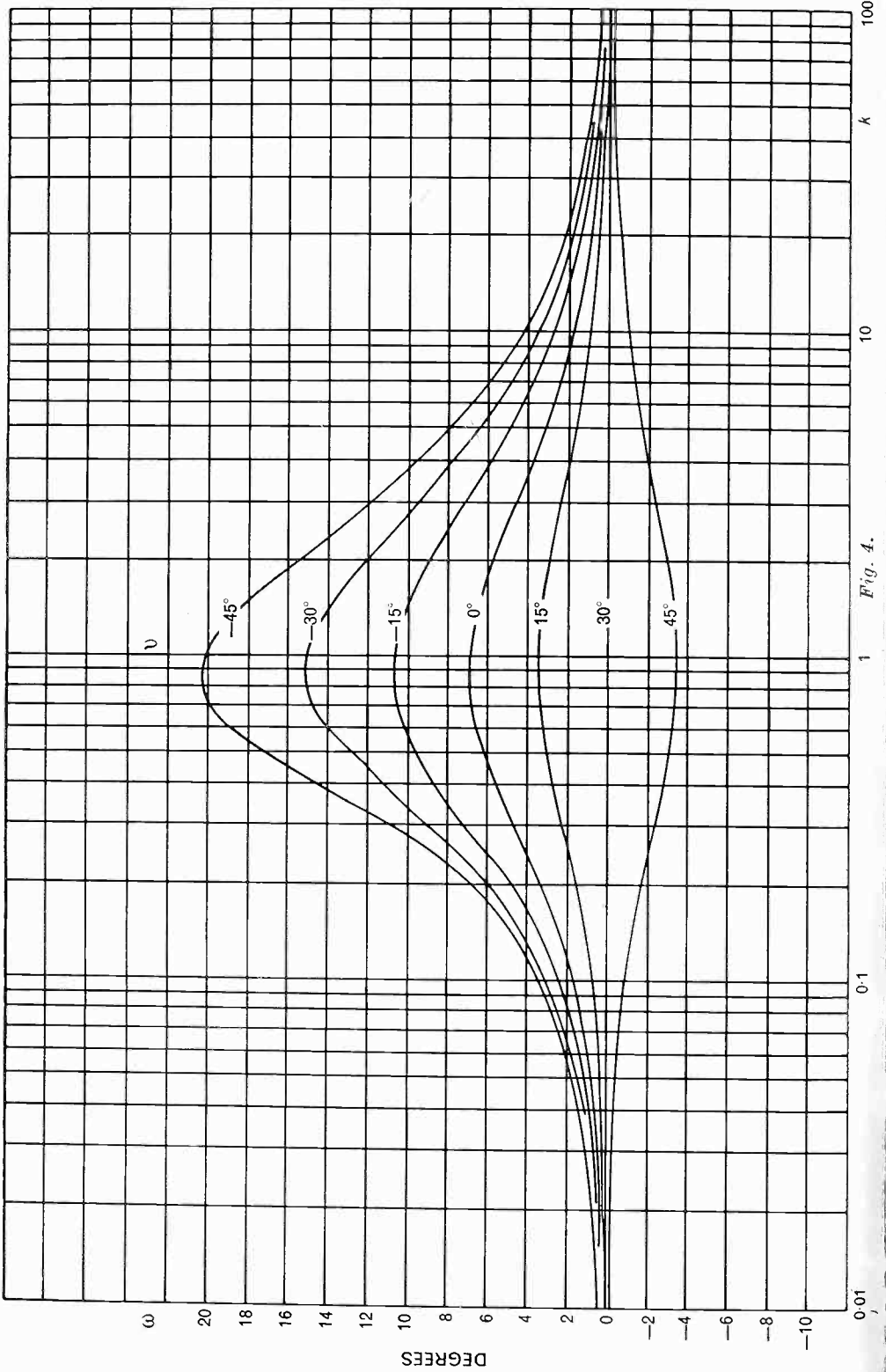


Fig. 4.

as $|\eta|$ is less or greater than unity. The author has in fact recently shown in some unpublished work that the complete Hankel form of the solution can be expressed in a modified inverse tangent equation which can be computed right through the transition region, whereas it is evident from the tables given by Norton⁽⁶⁾, and more recently by Jöhler, Walters and Lilley⁽⁷⁾, that the asymptotic expansions, which are extremely elaborate, yield only a very limited accuracy in this region.

This new tangent form of the solution is, however, relatively laborious to apply compared with the use of equations (7) and (16) and it therefore seems justified to present a set of curves based on this approximate but simple approach. If we write

$$\eta = |\eta| \exp(j\psi) \tag{18}$$

and

$$\zeta = |\zeta| \exp(jr) \tag{19}$$

then since ρ has already been defined as

$$\rho = |\rho| \exp(j\omega) \tag{20}$$

it follows from equations (4), (18), (19) and (20)

$$|\eta| = \frac{1}{k\sqrt{2}|\rho|} \tag{21}$$

and

$$\psi = \frac{\pi}{6} - r - \frac{\omega}{2} \tag{22}$$

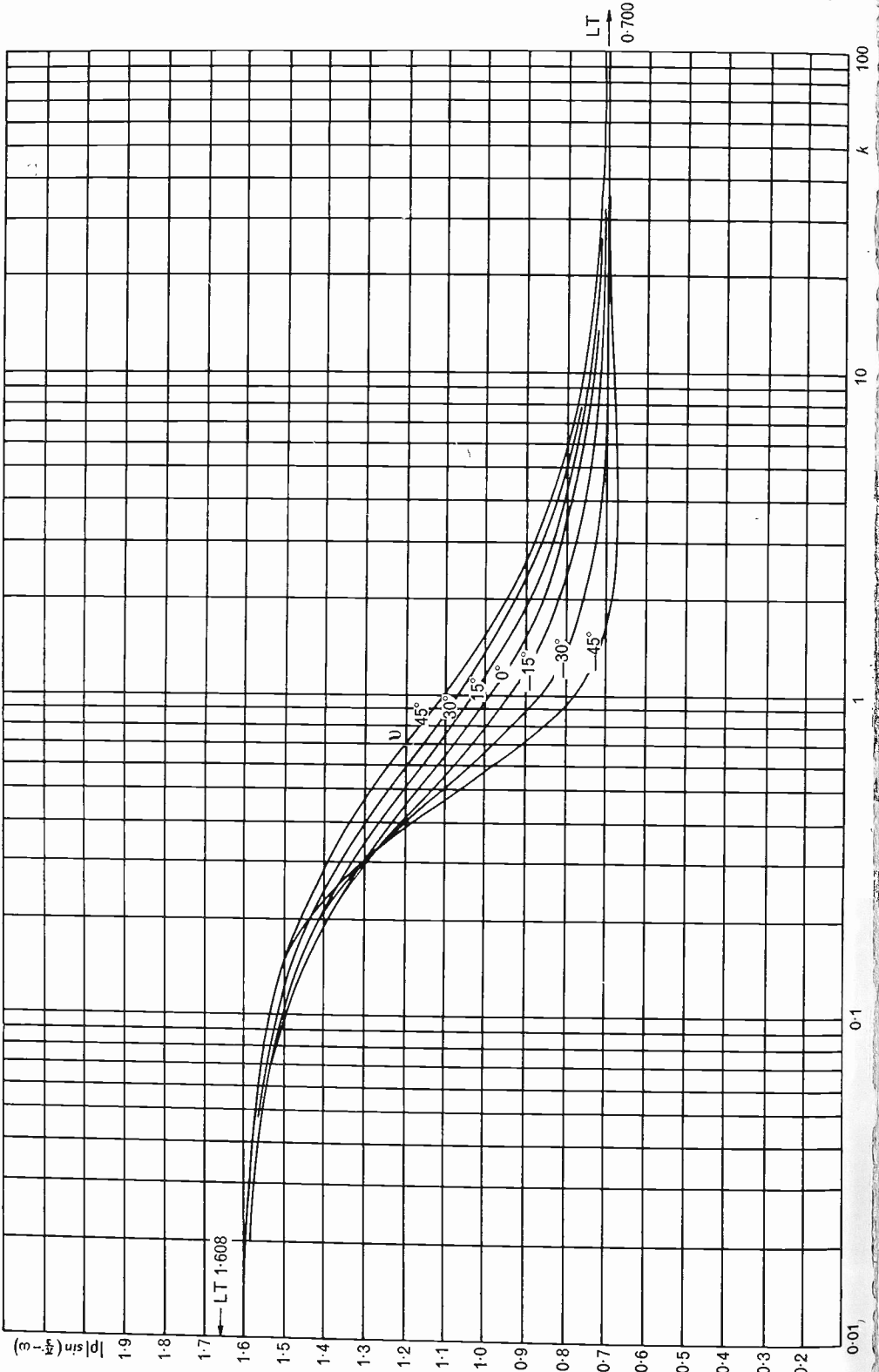
where

$$k = \frac{|\zeta|}{r^{\frac{1}{3}}} \tag{23}$$

For given values of r_0 , λ , ε and σ , x is known from equation (1) and $|\zeta|$ and v are known from equation (5) or equation (6), so that k is determined from equation (23); thus we can embrace all cases by solving equation (7) or (16) for $|\rho|$ and ω as functions of k for various values of v . From equation (5) we see that for vertical polarization v goes from 0 to $-\frac{\pi}{4}$ as λ goes from 0 to ∞ , and from equation (6) for horizontal

polarization v goes from 0 to $\frac{\pi}{4}$.

In the case of the earth we have for all practical values of ε and σ that is already effectively at its upper limit ρ_x for vertical polarization when λ is small enough to make $60\sigma\lambda$ no longer predominant over ε , while for horizontal polarization the value k attains at its maximum as λ is changed small compared with unity. Thus for vertical polarization the curve for



$v = -\frac{\pi}{4}$ largely suffices, while for horizontal polarization ρ remains effectively at its upper limit.

It is not obvious, however, that this state of affairs will exist when we consider the much smaller values of r_0 associated with hilltops. The eigen-value equation has therefore been solved over a range of k from 0.01 to 100 for values of v at intervals of 15° from -45° to 45° . Figs. 3 and 4 give the curves for $|\rho|$ and ω respectively. From these we have derived Figs. 5 and 6 for $|\rho| \sin\left(\frac{\pi}{3} - \omega\right)$ and $|\rho| \cos\left(\frac{\pi}{3} - \omega\right)$. The former is for use in equation (3) for α , while the latter is used in the calculation of the height quoted as approximately $50\lambda^{2/3}$ and shown in Fig. 1 and which is actually given by $r_0 x^{-\frac{2}{3}} |\rho| \cos\left(\frac{\pi}{3} - \omega\right)$. It also occurs in the expression for the phase velocity of the wave over the curved surface which is V given by

$$V = \frac{c}{1 + x_0^{-\frac{2}{3}} |\rho| \cos\left(\frac{\pi}{3} - \omega\right)}$$

where c is the velocity in free space.

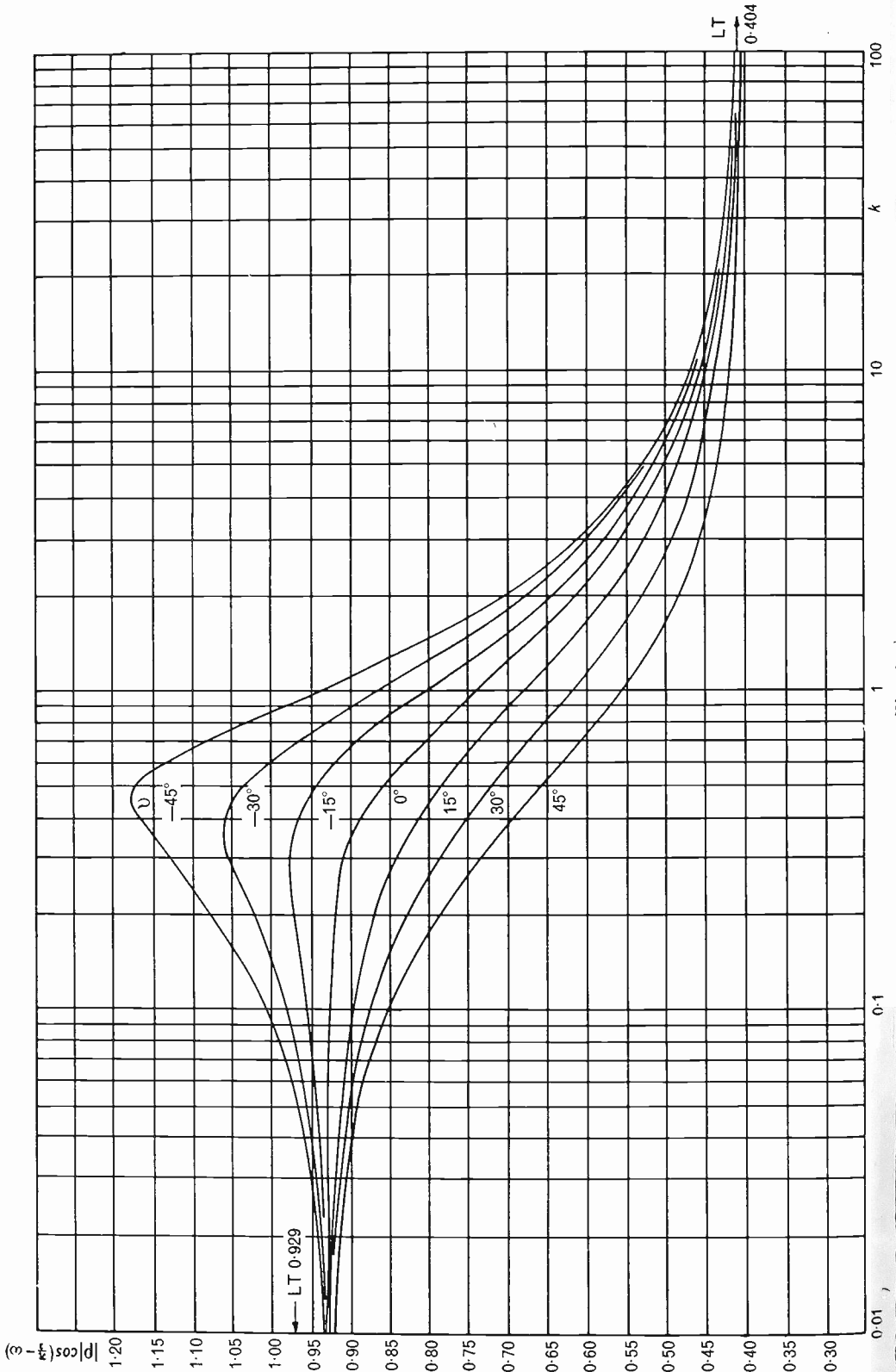
The curves for negative values of v agree well with those published by van der Pol and Bremmer⁽⁸⁾ and others. As far as the author knows, no curves for positive values of v corresponding to horizontal polarization have been published previously.

Some Examples and Discussion

To illustrate the use of the curves two examples will be taken. Consider first the diffraction of a wave with $\lambda = 10$ m. over a hill of radius $r_0 = 100$ m. so that $x = 20\pi = 62.8$ and $x^{\frac{1}{3}} = 3.975$. Assuming that $\epsilon = 2.5$ and $\sigma = 10^{-2}$ mhos per metre, we have from equation (5) that for vertical polarization $|\zeta| = 2.9$ and $v = -20.5^\circ$. Thus from equation (23) $k = 2.9/3.975 = 0.73$. From Fig. 5 we see that for $k = 0.73$ and $v = -20.5^\circ$, $|\rho| \sin\left(\frac{\pi}{3} - \omega\right) = 1.02$ as compared with the upper limiting value of 1.608 which it would effectively have for propagation round the curve of the earth for the same values of λ , ϵ and σ . Thus the value of α from equation (3) is $3.975 \times 1.02 = 4.05$.

From equation (2) the attenuation $\exp(-\alpha\phi)$ is equivalent to a decibel loss D given by

$$D = 8.686 \frac{\alpha}{r_0} \text{ decibels per metre} \tag{24}$$



and in the present instance this gives $\frac{8.686 \times 4.05}{100}$ i.e. 0.352 decibels per metre.

For horizontal polarization for the same conditions equation (6) gives $|\zeta| = 0.38$ and $v = 28.5^\circ$, so that $k = 0.38/3.975 = 0.0955$, whence from Fig. 5, $|\rho| \sin\left(\frac{\pi}{3} - \omega\right) = 1.52$. Then $\alpha = 6.04$ and $D = 0.523$ decibels per metre.

As a second example we will consider the diffraction of a wave with $\lambda = 1$ metre by a sea wave with an effective radius of 10 metres. This again gives $x = 62.8$ and with $\epsilon = 80$ and $\sigma = 4$ mhos per metre, $|\zeta| = 15.9$ and $v = -36^\circ$ for vertical polarization, so that $k = 4.00$ and $|\rho| \sin\left(\frac{\pi}{3} - \omega\right) = 0.70$. Thus $\alpha = 2.78$ and $D = 8.686 \times 2.78/10 = 2.415$ decibels per metre. For horizontal polarization $|\zeta| = 0.063$ and $v = 36^\circ$ so that $k = 0.0159$ and $|\rho| \sin\left(\frac{\pi}{3} - \omega\right) = 1.59$. Then $\alpha = 6.32$ and $D = 5.49$ decibels per metre.

In this case we have effectively the lower and upper limiting values for $|\rho| \sin\left(\frac{\pi}{3} - \omega\right)$ for vertical and horizontal polarization respectively, giving a maximum contrast in attenuation between them.

For horizontal polarization the largest value that $|\zeta|$ can have is about 0.5 corresponding to $\epsilon = 2.5$ on sufficiently short waves at the dielectric limit for propagation overland. For our condition that $\lambda < 0.5r_0$ the maximum value of $x^{1/3}$ is $(4\pi)^{1/3} = 2.324$ so that the maximum value for $|\zeta|$ is $0.5/2.324 = 0.215$, and the corresponding value of $|\rho| \sin\left(\frac{\pi}{3} - \omega\right)$ for $v = 0$ is 1.38, which represents the largest departure from the upper limit value of 1.608 we can obtain for horizontal polarization with the limitations imposed on the solution we have obtained.

In conclusion it should be remembered that the solution as applied to the effect of hills, etc., refers only to the signal strength at points within the shadow region. Moreover, as we have assumed that the first term of the diffraction formula is predominant, we can interpret this to mean that the distance beyond the horizon must be greater than that at which the attenuation associated with the second term is 10 decibels greater than with the first term. By considering the eigen-value equation for $s = 1$, we can show that this leads to the useful approximate criterion that the angle through which the wave is diffracted is at least as great as $x^{-1/3}$.

In terms of the distance d in equation (2) this gives $d \geq r_0 x^{-\frac{1}{3}}$, or in terms of $\alpha\phi$ from equation (3) that $\alpha\phi \geq |\rho| \sin\left(\frac{\pi}{3} - \omega\right)$. At the upper limit this implies that $\exp(-\alpha\phi) \leq 0.2$ and the attenuation is ≥ 14 decibels. Thus in applying the values derived above for attenuation in decibels per metre, the distance must be great enough to make the attenuation exceed 14 decibels if ρ is near its upper limit.

This restriction coupled with the condition that the curvature of the hilltops must be small enough to make $x \gg 1$ for the wavelength in question marks the border-line between the treatment of the diffraction loss in terms of decibels per metre round the curved surface and that in terms of Fresnel theory for an equivalent knife-edge. For a given position of a transmitter relative to an obstructing hill, this transition takes place as the receiver is moved further and further away and out of the shadow cast by the hill.

References

- 1 T. L. ECKERSLEY and G. MILLINGTON: *Phil. Trans. Roy. Soc.*, No. 778, CCXXXVII, pp. 273-309 (1938).
- 2 J. S. McPETRIE and L. H. FORD: *J.I.E.E.*, 1946, Vol. 93, Part IIIA, p. 527.
- 3 C. DOMB and M. H. L. PRYCE: *J.I.E.E.*, 1947, Vol. 94, Part III, pp. 325-339.
- 4 H. BREMMER, "Terrestrial Radio Waves." Elsevier Publishing Company, Inc. (cf. pp. 76-80).
- 5 S. MATSUO (1950), Report of the Electrical Communication Laboratory. Ministry of Telecommunication, Tokio.
- 6 K. A. NORTON, *P.I.R.E.*, 1941, Vol. 29, p. 623.
- 7 J. R. JOHLER, L. C. WALTERS and C. M. LILLEY, *N.B.S.*, Technical Note No. 7.
- 8 B. VAN DER POL and H. BREMMER: *Hochfrequenztechnik und Elektroakustik* 51 (6), pp. 181-188, 1938.

BOOK REVIEWS

TELEVISION EXPLAINED by *W. E. Miller and E. A. W. Spreadbury*
Price 12s. 6d.

This is a book which should interest the technically minded viewer or the electronics engineer who is not familiar with the special techniques and considerations which affect the design of television receivers. The man in the street would have to give attentive thought to the text and possibly some study elsewhere, but he should then be able to follow the explanations without great difficulty. Anyone with an electronics background could take it in his stride and be rewarded with a clearer insight into the whys and wherefores of the subject.

Although generally very readable, the style is a little peculiar in places with a tendency to tautology as for example: "... the oscillator frequency is higher than that of the signal frequency". A few technical points were noticed which need elaboration or correction. Of the three important differences between a video amplifier and an audio amplifier cited on page 85, the second - that a voltage output instead of a power output is required from the video amplifier - seems subsequently to have been lost sight of and no explanation is given of how

this difference affects video amplifier design. When describing the cathode-ray tube no mention is made of the units in which brightness is measured. Why are we expected to appreciate an EHT of 700 *Volts* but not a screen brightness of so many *Foot-Lamberts*? There is some confusion between current and voltage in the explanation of scanning in Chapter 10. The saw-tooth waveform in Fig. 61 is shown as "voltage or current" but is referred to in the text as the current waveform needed in the scanning coils. In the following paragraph current and voltage are intermingled in a fashion not strictly applicable. The statement on page 127 that critical damping is so-called because a resistance setting is critical, must be challenged. This is confusing two meanings of the word critical: *relating to a turning point or transition* on one hand and *precise* on the other. Finally one wonders what is con-

sidered "better" about the contraction μs for microseconds (page 144). An omission of some importance is any reference to slot aerials whether of the "chicken wire" or even simpler boundary wire type which have been found useful in fringe areas. This is possibly due to the fact that this type of aerial is more often used by amateurs than commercially.

On the whole, however, there is little to quarrel about. The presentation and printing are excellent; the numerous diagrams are well drawn and, in general, conform to accepted standards. The reproductions of photographs taken from the television screen serve admirably to show the effects of various maladjustments.

Published at a reasonable price of 12s. 6d. this book is good value and one is certainly left with the feeling that, from the receiving viewpoint at any rate, one has had television explained.

ENCYCLOPEDIA ON CATHODE RAY OSCILLOSCOPES AND THEIR USES

2nd Edition by *John F. Rider and Seymour D. Uslan*

John F. Rider, Publisher, Inc, New York. London: Chapman and Hall Ltd. Price £10 10s.

This monumental work, containing nearly 1,500 quarto pages, purports to present, in one volume, "a cross section of cathode ray theory, as well as applications in all the fields of research where this most versatile device can be used." Leaving aside, for the moment, the questions to whether cathode rays are devices and, indeed, whether the authors really mean what they say, the book does present, in one expensive and rather unmanageable volume, an extremely comprehensive survey of cathode ray oscilloscope theory, design and application. Such a book could not have been produced cheaply; it might have been produced in a more convenient form.

After twelve chapters devoted to theory, construction circuitry and operation of oscilloscopes, chapters thirteen to twenty are devoted to applications and measurements of all kinds, including medical investigations and photographic apparatus testing. The photography of oscilloscope traces is also adequately treated.

Next follow eighty-six pages of pictures of complex waveforms, with varying harmonic contents. These might surely have been omitted from the main book as might over-

two hundred pages devoted to circuit diagrams of commercial oscilloscopes. Most of these are of American manufacture which have a limited use in Great Britain. If these two last sections had formed a separate volume, both would have been more manageable.

The subject matter is, on the whole, extremely well treated, though the scope of the work forbids much detail in any one section. The authors obviously are experts in their field, and the treatment of most subjects is clear and accurate.

A number of misstatements or misprints occur, as must be expected in such a work. Deflection and Deflection Sensitivity have been mixed up on pp. 3-4. Oscilloscope traces cannot be electrical quantities (pp. 3-25). The equation for Z_1 on pp. 13-24 is wrong and what an angle of $K - 20$ is (pp. 19-31) is anyone's guess. Apart from such faults as these, the printing is excellent and the diagrams clear and well drawn although standard symbols for valves and the like might have been used in all cases.

For those who can afford it, the book is highly recommended and certainly should find a place in the library of any concern which might use cathode ray oscilloscopes.

AN EXPERIMENTAL SCAN CONVERSION SYSTEM FOR THE PRODUCTION OF BRIGHT RADAR DISPLAYS

By D. L. PLAISTOWE, A.M.Inst.E.

The following article describes work carried out with an experimental Radar Scan Conversion System. A twin-gun tube, type TMA 403X manufactured by C.S.F., was used for the investigation. By its means Radar video signals are written as a charge pattern on a storage electrode within the tube. This is scanned by an electron beam in raster fashion, the resultant video signals then being used to modulate a standard television cathode ray tube. Thus a Radar PPI display can be viewed in normal ambient room lighting conditions. The resolution was found to be greater than that obtainable from an alternative bright display, namely the "Direct View Storage Tube."

Introduction

In an early attempt to produce bright radar displays an orthicon television camera was used to televise a normal PPI having a fluoride screen. The video signals were then displayed on a 405 line television monitor. An improved version of this "visual transducer" uses one of the new transparent phosphor tubes, having high resolution and short persistence. Radar signals appearing on the screen are televised by a camera tube known as the "Storage Orthicon." By this means the video signals produce echo trails on a bright TV type display tube. As far as is known, no work on this system has been carried out in this country.

A third means for producing a bright display makes use of the "Direct View Storage Tube." No television intermediary is required in this case. Development work is still proceeding in this country and in the U.S.A. on this system, particularly to improve aircraft-cockpit radars.

A fourth method makes use of a so-called "Intermediate Charge Storage Tube" of the co-axial double-ended type. This enables signals to be written in polar co-ordinate form and stored on a disc shaped target within the tube. A television raster is used to read off the information in the form of video signals. Thus, through scan conversion a bright "Kinescope" tube of short persistence can be used to display the radar echoes.

A converter tube of the type known as the TMA 403X, made by C.S.F., has been used experimentally (Fig. 2). The television 625 lines, 50 pps interlaced, Continental Standard was adopted for reading and display purposes. Fig. 1 shows the equipment employed for the experiments.

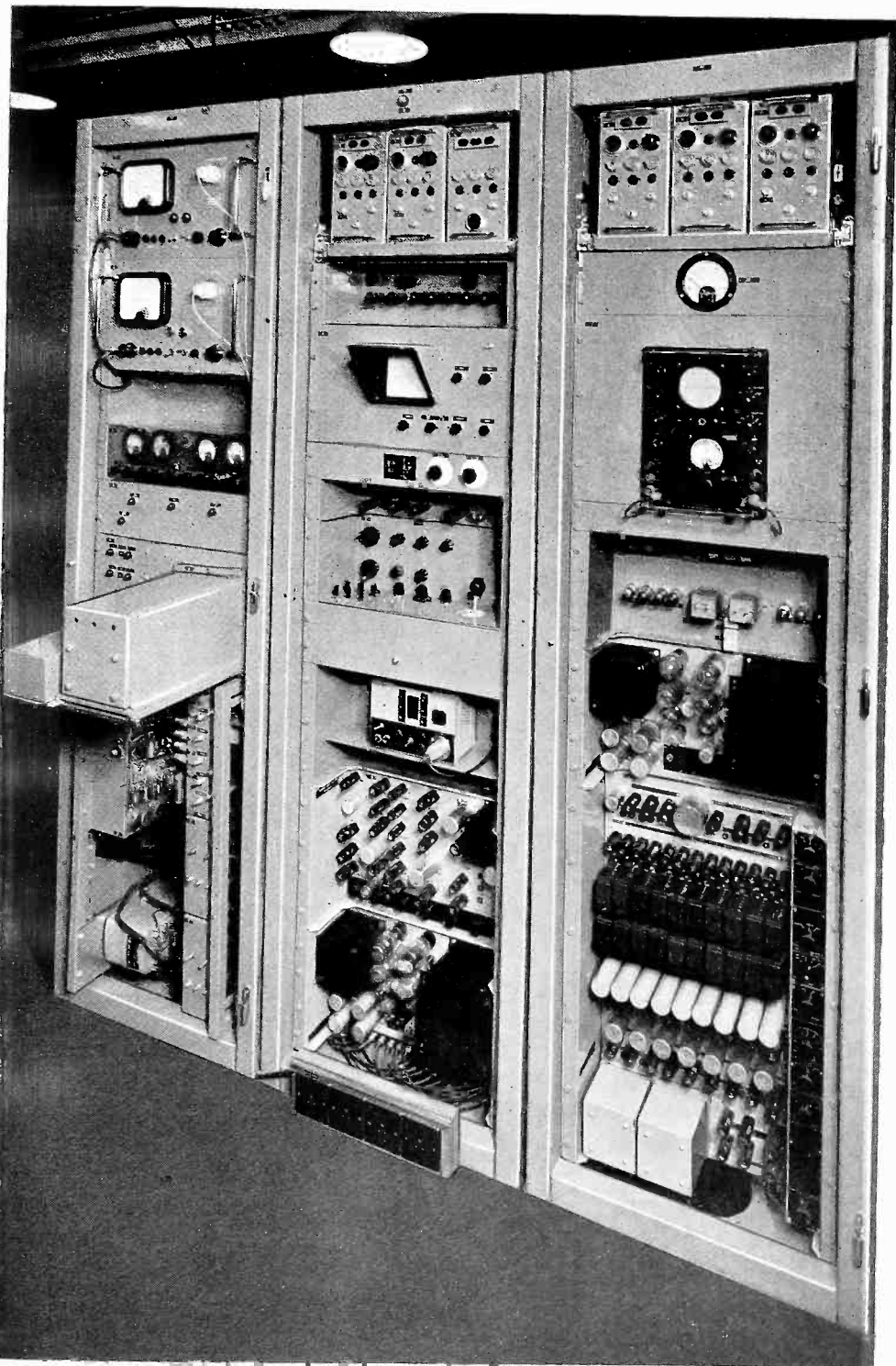


Fig. 1.

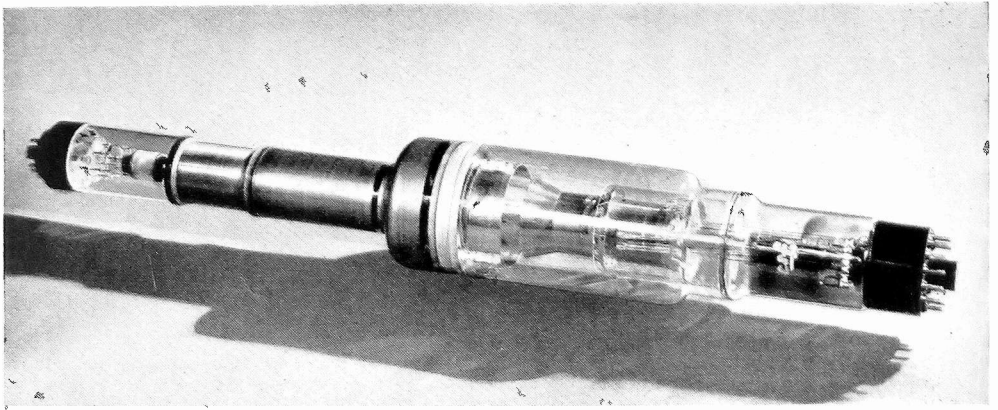


Fig. 2.

The high-velocity writing beam of the tube is modulated by echo signals and scans one side of the storage target. Thus a charge pattern proportional in strength to the echoes is written and stored. Figs. 2 and 3 show the arrangement of the electrodes.

Owing to "bombardment induced conductivity," charges reach the back surface of the thin insulator which is a part of the target. A reading beam of low velocity, scanning that surface in television raster fashion, gives rise to the emission of secondary electrons. These proceed to an annular collector output electrode connected to an amplifier. Wherever an echo charge has been written the output secondary current is greater than that at the reading datum level. By a suitable choice of operating conditions of the reading gun the secondary current, time quantized by the raster scanning action of the beam, can be made small. Thus a large number of copies of the radar echoes can be read off before the charge has been neutralized. Suppose, for instance, that 2,250 reading scans occur before the written signal is completely erased. Then, with a reading repetition rate of 25 frames per second and aerial rotational velocity of 4 r.p.m. the final display will show six successive echo paints. This ensures that a "tail" of suitable length will be obtained. This type of tube thus enables normal television-type kinescope tubes to be used for radar displays. The reading raster, however, introduces normal television scanning errors and causes diagonal lines to be broken up.

The TMA 403X is capable of a resolution of 400 lines. The present 625 lines system thus imposes no significant additional limitation.

Experimental Work

SCREENING THE TUBE FROM EXTERNAL MAGNETIC AND ELECTROSTATIC FIELDS

During the preliminary experiments the TMA 403X was merely mounted horizontally on a tray inside a mu-metal screening box. By this means

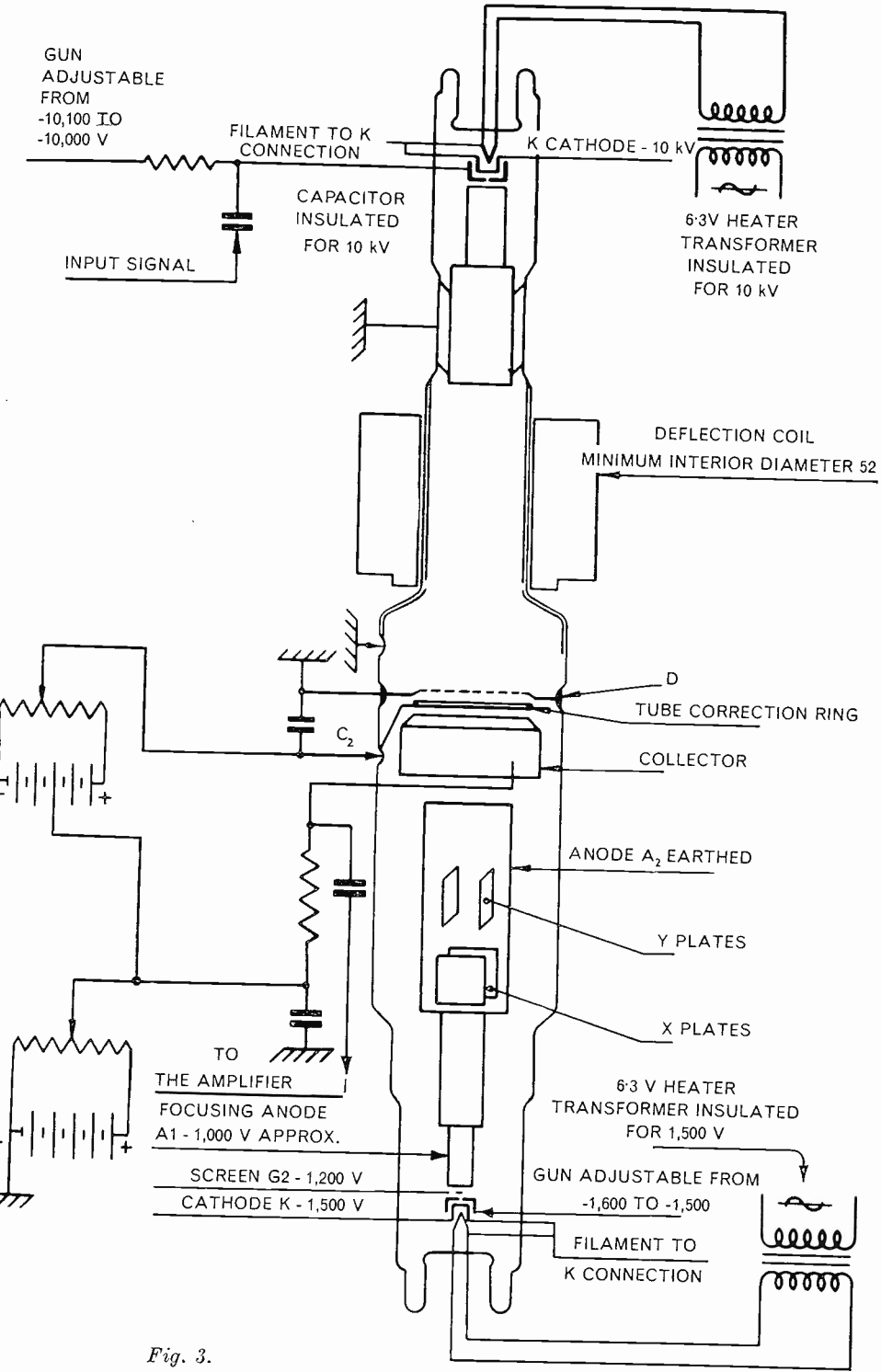


Fig. 3.

disturbances by time varying fields in the equipment, or static deflection due to the Earth's field, were reduced in the usual manner. The results obtained were still unsatisfactory, however, due to crosstalk within the tube itself, and additional precautions had to be taken.

CROSTALK BETWEEN WRITING AND READING SCANS

Polar co-ordinate scanning is used on the writing side of the target, the writing yoke being fitted around the neck of the tube, as shown in Fig. 3. An electrostatically deflected reading beam scans the back surface of the target in television raster fashion. The tube was at first operated without screening in order to ascertain the magnitude of electrostatic crosstalk between writing fields and reading beam.

It was found that the picture on the monitor was distorted and unstable. One disturbance effect appeared to be confined to five bars which moved either up or down the raster on the monitor. This was most obvious when the TV sync. pulses had been added to the video.

Echo signals were moved in roughly circular loci on the screen as the disturbance bars moved through them. The rate and direction of movement were related to the mains-locked field frequency and the free-running 250 scan sweeps.

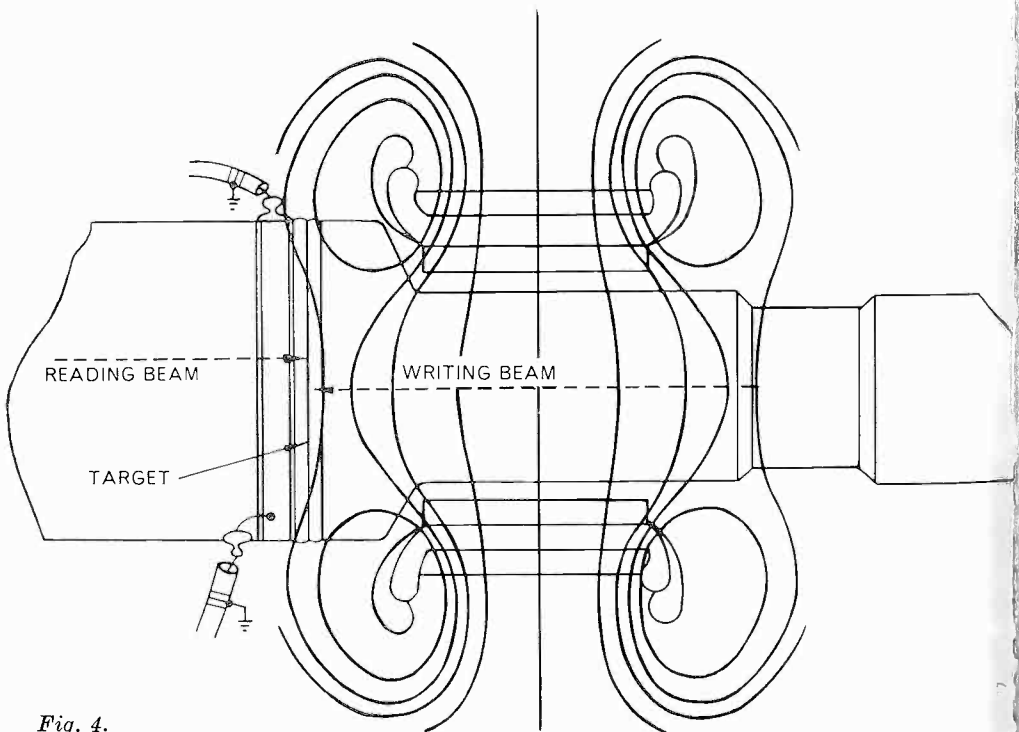


Fig. 4.

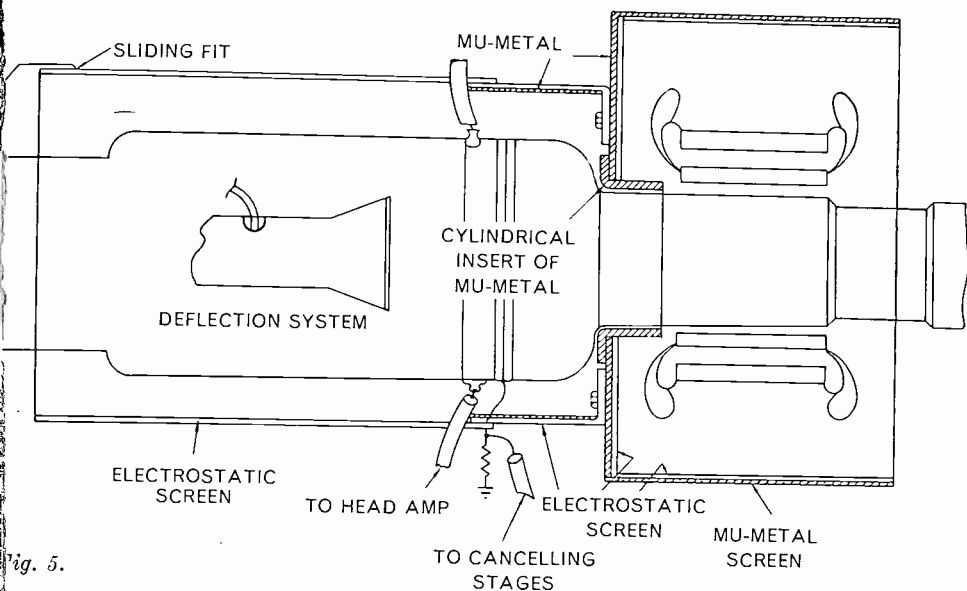


Fig. 5.

The disturbances waxed and waned in severity, as would be expected if the writing fields were responsible. This would be due to the changes in amplitude of the sine and cosine fields, four times per revolution of the resolver. In fact it was found that the effects ceased when the writing scan was switched off.

THE PREVENTION OF CROSSTALK

Reference to Fig. 4 shows the probable linkage that existed during the first test. Fig. 5 shows the rather elaborate screening used to avoid distortion of the reading raster on the target. The mu-metal cylinder was fitted with a screen off the lines outside the yoke in the usual manner. A mu-metal gate was fitted at the end of the cylinder close to the reading beam. This screened off the end field of the yoke, and also the cross fields due to the end turns of the coils.

A further improvement resulted after an additional mu-metal lined concentric cylinder had been fitted over the target as shown. By this means magnetic leakage, and consequently spurious deflections were reduced. The effect, however, was still too great to be tolerated, and it was obvious that remaining leakage fields were confined within the tube.

Finally a short mu-metal cylinder was fitted inside the main cylinder as shown. Care was taken to ensure that a shorted turn effect did not overload the scanning system. This simple device enabled more effective tapping of the ends of the interior magnetic lines to be effected. The writing scan field was thus confined to the writing end of the tube.

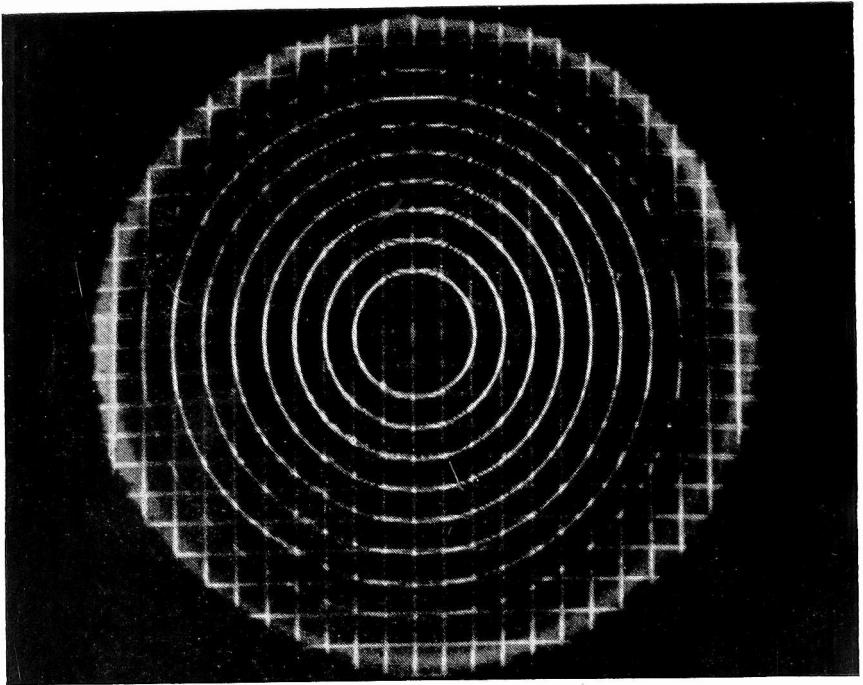


Fig. 6.

Distortion of the reading raster was then found to be insignificant, and the bar effects moving up the raster were seen to be greatly reduced.

Another effect was found to be due to flyback pulse crosstalk between the writing scanning field and the reading head amplifier. This was greatly reduced by improved screening of the reading circuitry.

The performance of the tube was checked by means of a high-grade 14 inch television monitor. Satisfactory synchronism was then secured, using normal combined signals over a co-axial cable. Separate drive syncs. were then used to cross-check the performance. The results were also assessed by displaying them on a 21 inch monitor Type 5369A. By means of the larger display, working on composite signals, small errors became more obvious and were eliminated by further work.

TELE-RECORDING SCAN-CONVERTER VIDEO SIGNALS

Reading signals were applied to a tele-recorder, and images from positive prints on 16 mm. film were afterwards projected on to a 6 foot \times 4 foot 6 inches screen. This method of recording was found to be suitable for the production of large displays.

Range ring pulses from the radar equipment were stored, and the resultant ring on the monitor checked against a circle marked on the face. The dimensions of the reading raster were next adjusted so that the vertical diameter of the image of the storage disc just filled the height of

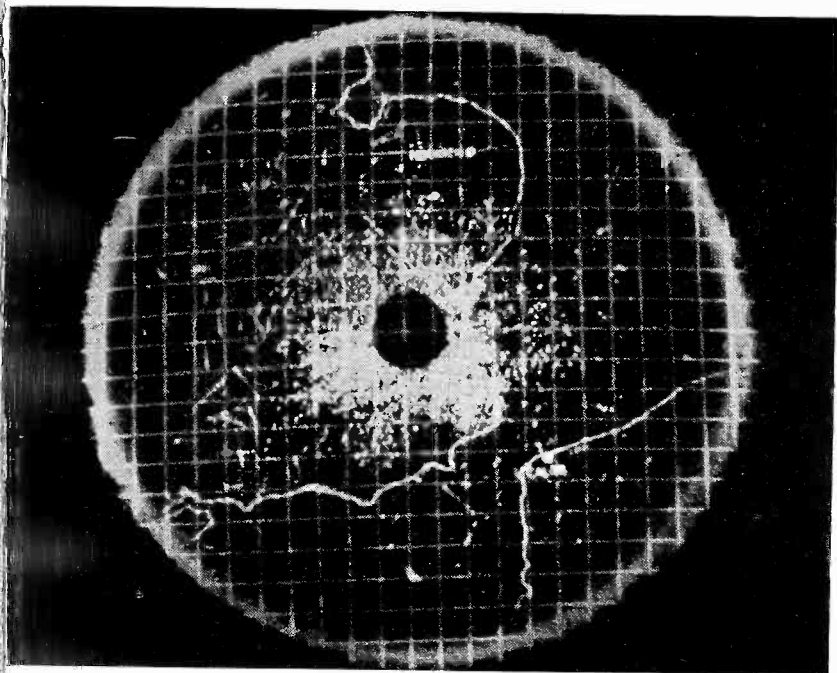


Fig. 7.

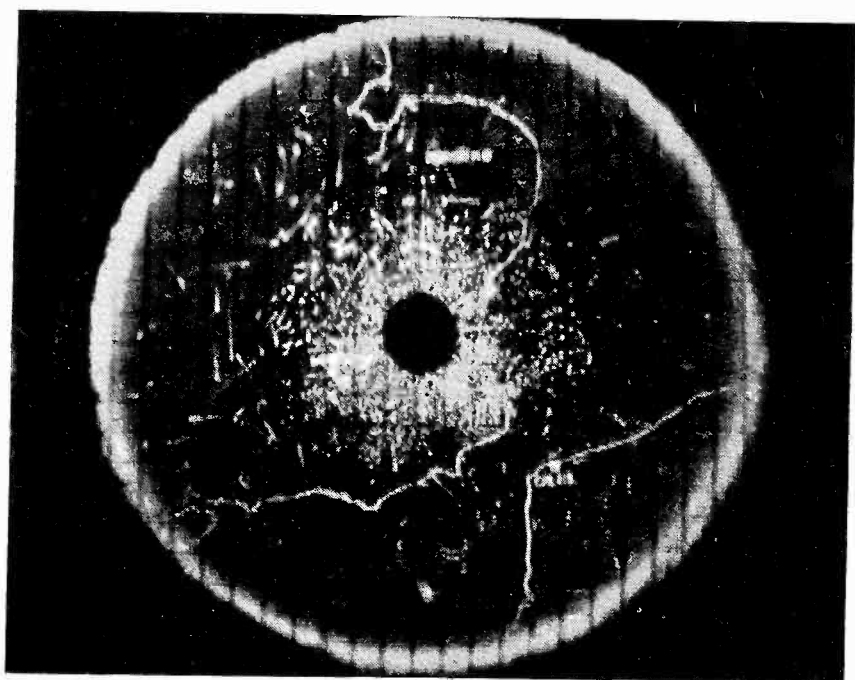


Fig. 8.

television camera tube. Feed back, aperture correction, gain control and signal polarity are adjustable in each amplifier. The separate outputs were taken to the cancelling stage shown in Fig. 11. The polarity of the signal from the mesh, on the grid of V1b, is negative, and the spurious signal positive, therefore at the anode the wanted signal is positive and the spurious negative. The polarity of the signal and spurious pulses is negative from the collector electrode of the scan converter tube. The waveform is amplified and the polarity of the input signal and spurious pulses at V1a grid is positive. The pulses therefore make the cathode of V1b more positive, and the anode volts rise during the incidence of wanted pulses. The signal pulses are in phase with those due to the grid excitation of V1b, but the spurious pulses are in anti-phase and tend to cancel. Suitable adjustment of the input level of signals to V1a and V1b, from both amplifiers, enables this to be effected and the output from V1b is applied to V2a. Cathode correction of V2a ensures that the frequency response is maintained. The output level is suitably adjusted before the signal is applied to the video and blanking signal mixing unit. This is used in the same way as in a television camera chain. The display shown in Fig. 12, taken a short time after Fig. 9, shows complete elimination of the spurious signals generated by the tube. If the radar signals have been differentiated negative excursions must be removed by bottom limiting.

The cancelling stage V1a, V1b, is described in a French patent⁽³⁾ and is there shown connected directly to the tube electrodes. If this were to be

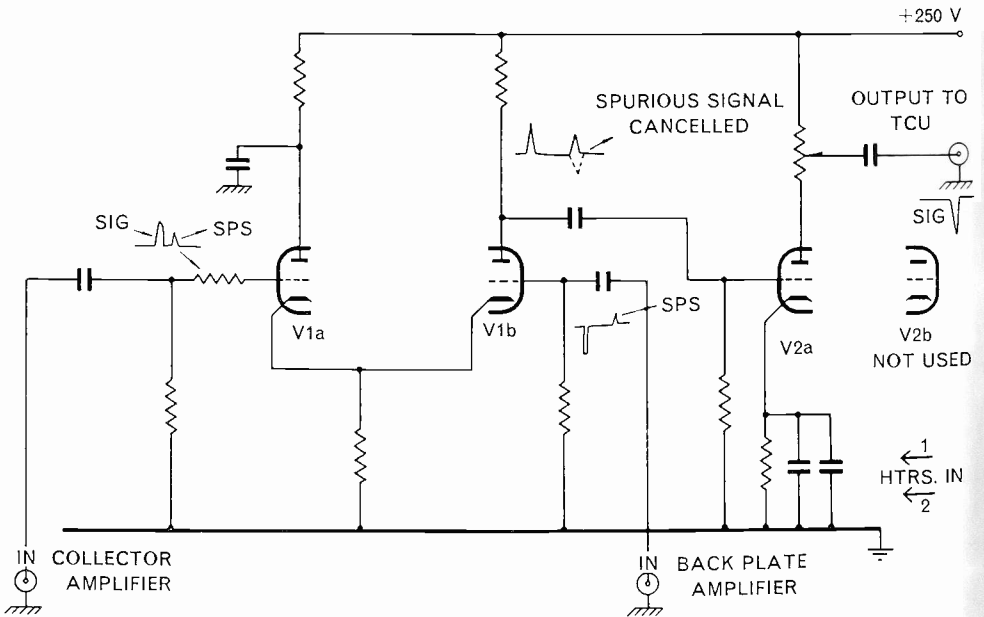


Fig. 11.

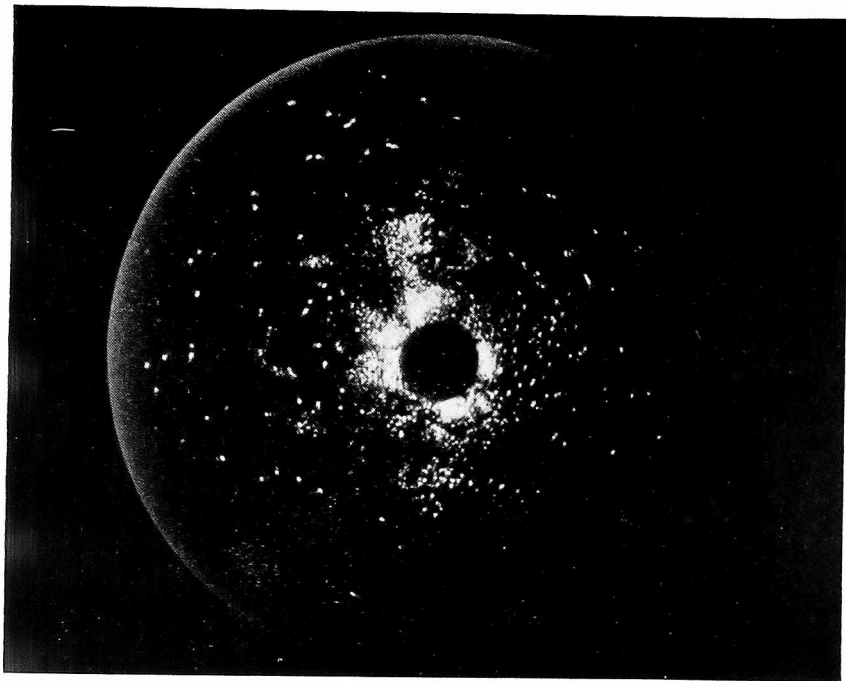


Fig. 12.

In the case in practice, the input signals to be cancelled would be at the millivolt level. In the system described above, cancellation takes place at approximately the 2 volt level.

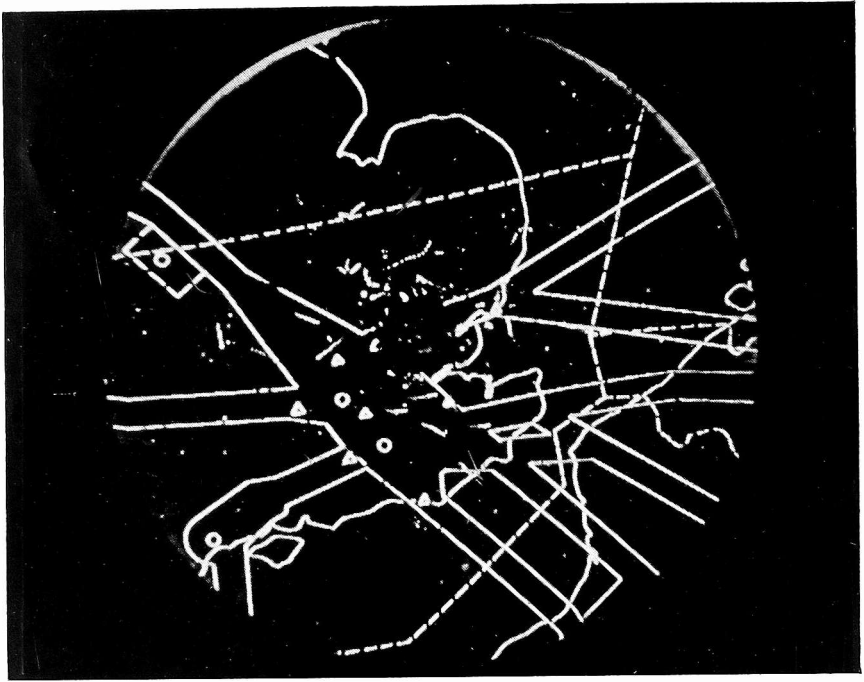
SPURIOUS SIGNALS GENERATED BY THE READING BEAM

In practice the reading raster is made to scan the whole of the circular target. This implies that beam electrons also scan other objects outside the diameter of the target. These emit secondary electrons which proceed towards the collector electrode.

Firstly the rim of the target supporting the insulator surface can give rise to an output signal. Thus a bright annular ring appears around the display, shown in Figs. 6, 7 and 8. Other rings can also be observed due to overscanning the target. Means for avoiding these effects have been described in a British Patent Specification⁽²⁾.

DISTORTION OF WEAK ECHOES DUE TO NON-LINEARITY OF THE WRITING GUN

When the gun was operated with low bias on the grid, echo images on the display tended to be obscured by stored noise. This persisted during approximately half of an aerial scan in azimuth. If the writing gun was biased back to prevent storing the noise, some of the weaker signals were not stored either. This was avoided by employing current feed-back to the writing gun cathode. Undue blooming of the spot by the strong

*Fig. 13.*

signals was also minimized by this means. Thus it became possible to differentiate more readily between 2μ sec. (Fig. 13) and 5μ sec. radar echo pulses (Fig. 14). The results are better than those obtained from a Direct View Storage Tube displaying 2μ sec. pulses under similar conditions (Fig. 15). When the latter was taken, a 3 inch display was used. Figs. 13 and 14 were photographed directly from the face of a 21 inch tube.

A SECOND SPURIOUS EFFECT PRODUCED BY THE TUBE WHEN SIGNALS ARE BEING WRITTEN

After an aircraft echo signal has been written on the storage surface the monitor spot image at first appears grey. Some seconds then elapse before it reaches optimum brightness. During the next aerial scan the aircraft echo will be written in a different position. Therefore, as no further integration occurs the brightness will not reach a maximum. On the other hand a permanent echo, or parts of cloud signals being re-written, produce greater charges, due to integration. The cloud response at first turns dark grey or black, as before, but due to the greater charges, the brightness slowly increases to a maximum (Fig. 16). This is described below. Phenomena occurring within the target insulator during the process of writing include that of "bombardment induced conductivity." Thus, the ionization of molecules in the path of the beam give rise to space charge polarization of the insulator. Moreover, at the same time, as previously

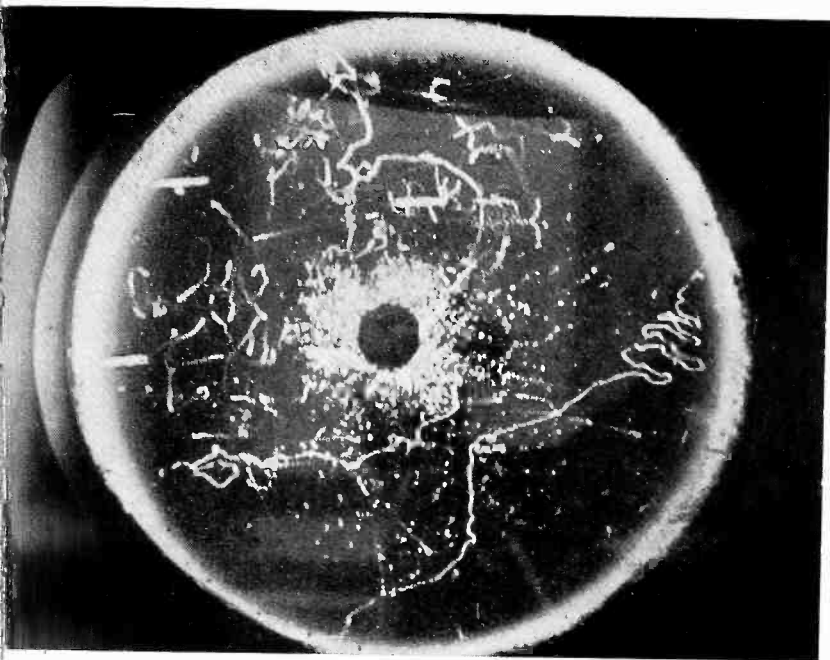


Fig. 14.

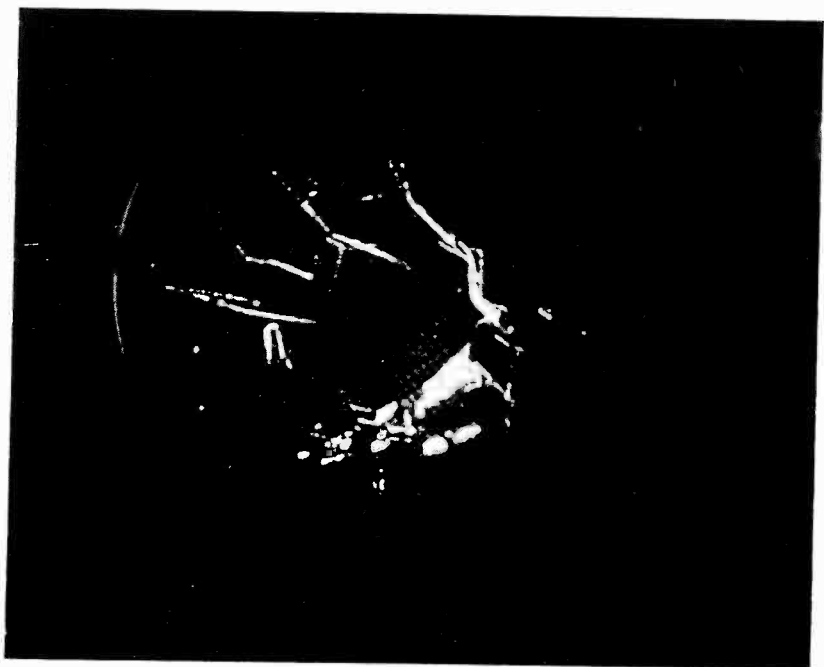
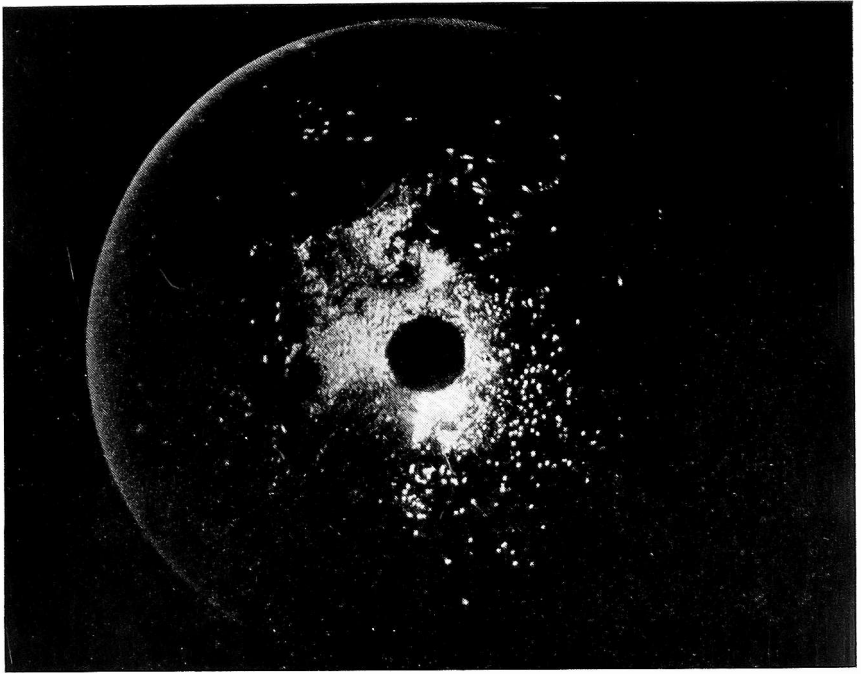


Fig. 15.

*Fig. 16.*

explained, some electrons escape from the surface; these cause the spurious signals which have to be cancelled as described. The build up of charge in the 0.5 micron thick storage insulator is also found in other materials under similar conditions. The resistance of the insulator between front and back surfaces is momentarily lowered, due to the action of the writing beam.

The reading beam at first tends to leak through the insulator, therefore for a short time after inscription full secondary emission does not occur. This is responsible for the initial reduction of brightness of the display. The effect can be minimized at the expense of storage persistence by increasing the reading current.

THE MEASUREMENT OF CLOUD VELOCITY

It was observed that the edge of drifting cloud does not appear to be momentarily reduced in brightness to quite the same degree as those parts being overwritten. Furthermore, the main part of the cloud looks brighter because charges previously written are integrated.

It would appear that tubes designed to augment this effect would prove to be of future use in meteorological work. The cloud velocity would be ascertained by measurement of the distance between the new edge, and that written during the previous aerial scan (Fig. 17).

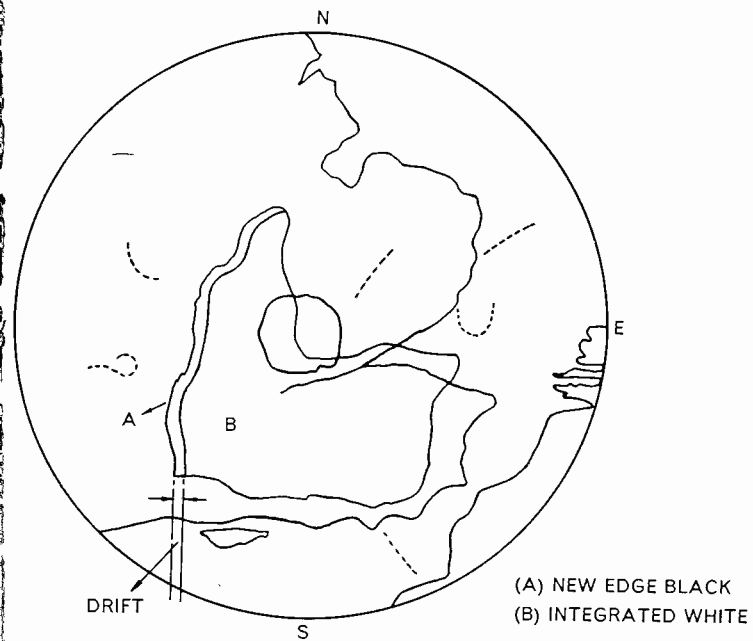


Fig. 17.

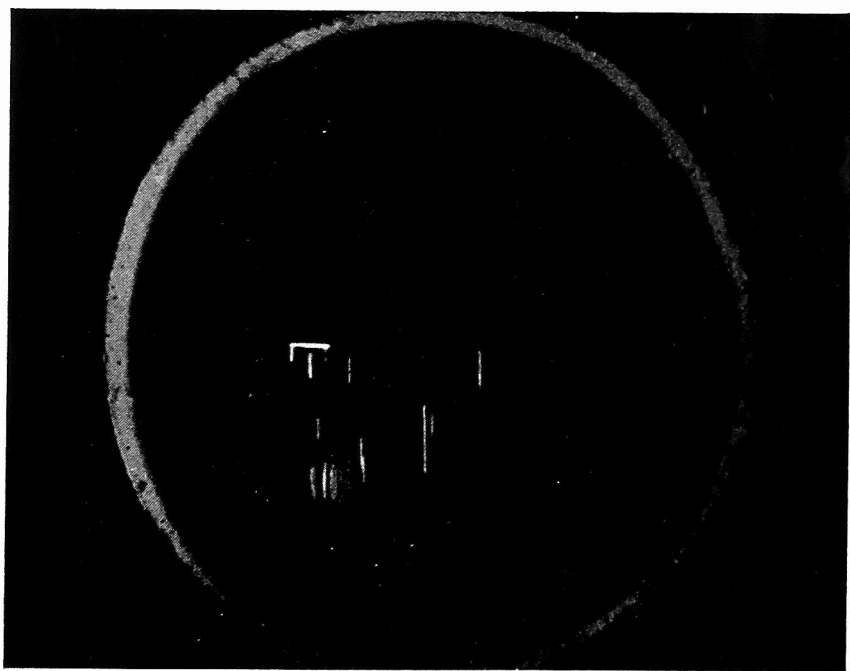
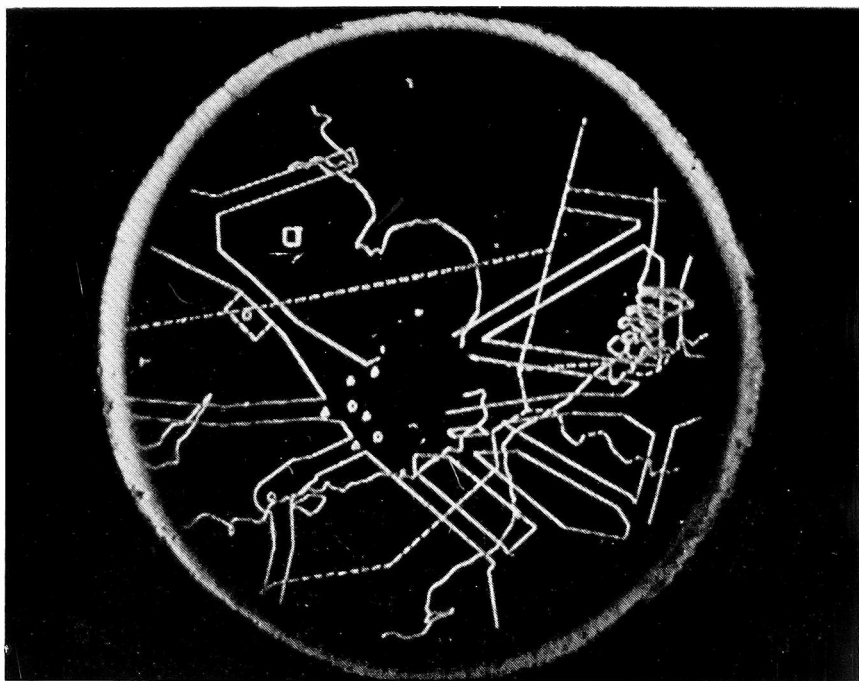


Fig. 18.

*Fig. 19.*

THE PERSISTENCE OF RADAR ECHO TRAILS

Results obtained from two specimens of the TMA 403X differed as regards the duration of the stored signals. No. 1 enabled long echo trails to be painted as seen on Fig. 14. No. 2 gave slightly better definition and a reduction of the white spurious annular ring. The duration of charge storage however was inadequate for normal Radar PPI, but good Height Finder Displays were obtained (Fig. 18). In this instance the time interval between successive sweeps of the writing gun is much less than in the case of the PPI.

THE SCAN CONVERTER USED FOR HEIGHT FINDER DISPLAYS

The Height Finder Display produced by the equipment was comparable to the PPI in brightness.

It was found advantageous to adjust the tube electrode potentials to enable moderate persistence of the vertical bars to be achieved. This enabled quicker erasure to be effected when changing the direction of scan in azimuth.

INTERCONSOLE MARKING ON RADAR SCAN CONVERTER DISPLAYS

Symbols for marking echoes were derived from circuitry triggered by line and frame frequency sync. signals. A square-shaped symbol produced by this means is shown on Fig. 19, placed close to an echo on the airplane map

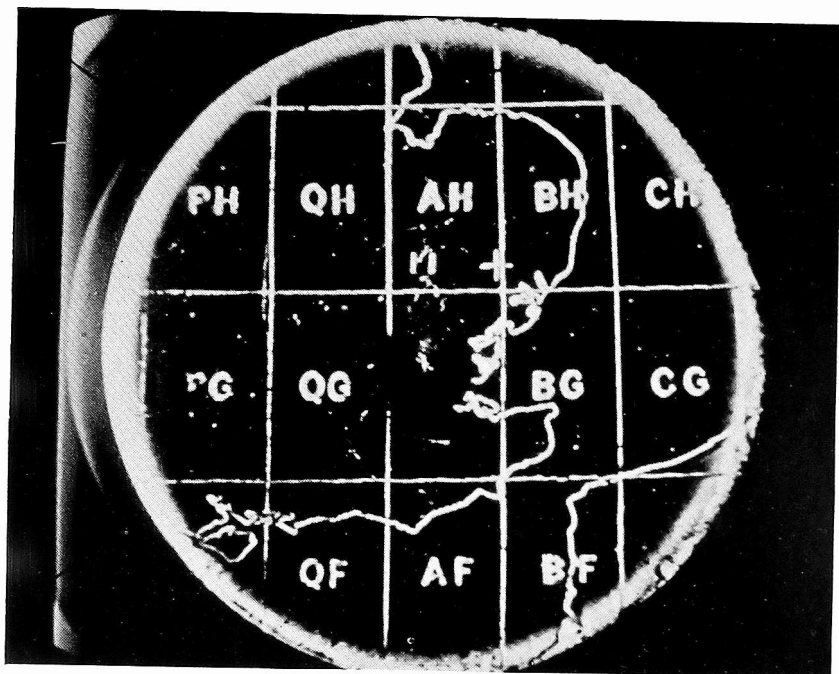


Fig. 20.

produced by video mapping. Fig. 20 shows a display upon which is a different symbol, namely two vertical bars. It and others were produced by altering the circuitry as required to delete parts of the square. This was done by operating appropriate push buttons. Any one of these symbols could be sent to all the co-operating displays, and also to a height finder as shown on Fig. 18.

Remarks on the Future Development of the Scan Converter

It would seem desirable to:

- (a) Improve the structure of the display presentation.
- (b) Reduce stepped edge effects due to scanning diagonal lines by the television raster.
- (c) Increase the resolution.
- (d) Reduce inter-frame flicker.

One approach to the solution of these problems may be as follows:

Some time ago experiments in a different field, namely closed-circuit TV film recording, used isochronous spot-wobble for similar purposes⁽⁴⁾. This technique must not be confused with normal spot-wobble as applied to some television sets. The latter technique would be quite unsuitable. Line-wave deflections were applied to the scanning system of the film scanner. Similar deflections exactly in phase were also used to wobble the lines of the monitor display. The amplitude of the wobble was adjusted to

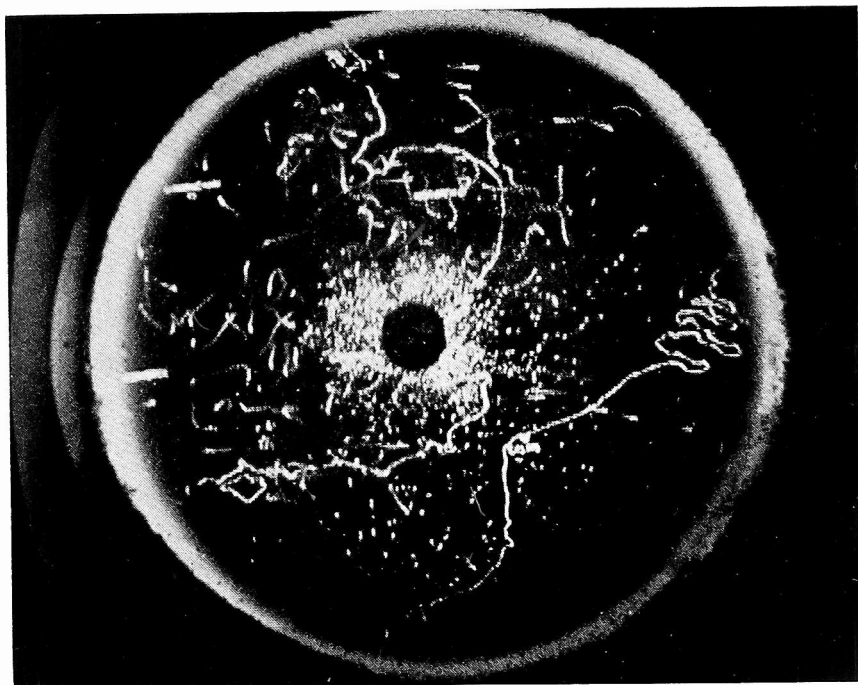


Fig. 21.

fill in the gaps between the lines. This improved the apparent structure of the picture without requiring an increase in the number of lines. Raster effects produced when scanning across diagonal lines of a display became less obvious (Fig. 22) and the resolution was improved.

It was thought that if isochronous spot-wobble were to be applied to both the reading scan of the converter and of the monitor similar improvements might be obtained. Thus the stepped edges as seen in Fig. 21 would be avoided. A further advantage might be a reduction of apparent line

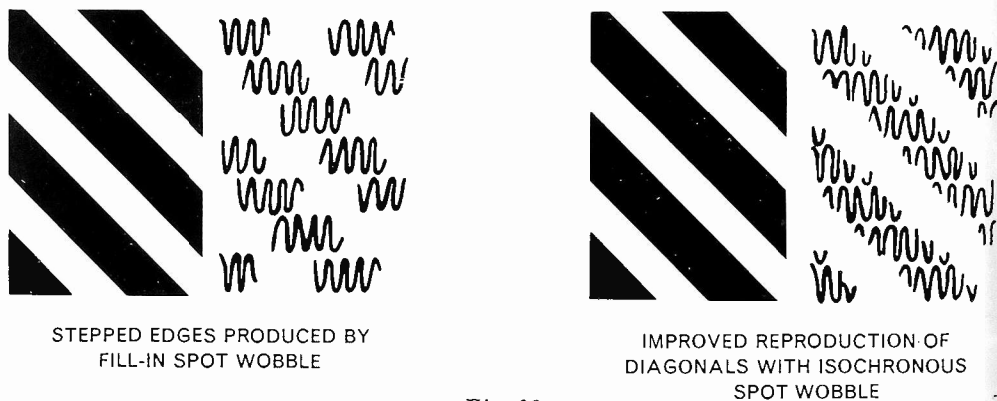


Fig. 22.

precession which is due to the use of interlaced scan. Eyestrain due to prolonged viewing of fine detail, which also makes line precession most obvious, would be reduced, and inter-field flicker would be less obvious.

Preliminary tests have in fact indicated that at least two of the expected improvements would be realized, namely reduction of stepped edge effects, and precession. A method of applying this system to scan conversion in cases where the displays are some distance apart has been devised.

This system is capable of increasing the resolution without requiring an increase in the number of lines. Thus a 625 line system provided with amplifiers of greater bandwidth might produce results approaching those obtainable from a conventional display.

The Association of Bright Plan-Position and Height Finder Displays

The use of two tubes in a converter system would enable bright PPI and Height Finder Displays to be obtained. These could be viewed together in ambient lighting normally used for viewing television displays. Some economy of circuitry could be achieved, the television waveform generator, raster generator, and EHT generators being common to both tubes.

Acknowledgements

The Author wishes to thank the Chief of Research for permission to publish this article and is indebted to colleagues of the Radar Display and Data Handling Laboratories, Television Development Group, Television Test Department, and Photographic Research Section, for their assistance in this work.

References

- Brit. Pat. No. 858475. M.W.T.Co. and Author.
- Brit. Pat. No. 857271. M.W.T.Co. and Author.
- French Pat. No. 724293. C.S.F. and M. Touslemond.
- Brit. Pat. No. 758085. M.W.T. Co. and Jesty and Sarson.

Bibliography

- LECOMPTE: "Towards Visual Air Traffic Control," *British Communications and Electronics*, March 1958.
- D. LIPMAN, D.F.C.: "Some Problems in the Display of Information for Air Traffic Control." *British Communications and Electronics*, March 1959.
- Phys. Review* 1949, pp. 472-478.
- Ziel Tech. Phys.*, pp. 307-313, 1938.
- BRUINING and J. H. DE BOER: *Physica Haag*, 6, P. 834.
- BRUINING: "Die Sekundärelektronen-Emission fester Körper."
- KNOLL and B. KAZAN: "Storage Tubes and their Basic Principles."
- PENSAC: "The Graphecon," *R.C.A. Review*, March 1949.
- PENSAC: "The Metrecon," *R.C.A. Review*, June 1954.
- LAHL: *Zeit. Tech. Phys.*, pp. 559-563, 1937.
- WARNECKE: *L'Onde Electrique*, pp. 509,540, 1937.
- Phys. Review* 1950, pp. 248-257.

BOOK REVIEW

PRINCIPLES OF SERVOMECHANISMS *by A. Tyers and R. B. Miles*

Sir Isaac Pitman & Sons. Price 25s.

This book sets out to be a primer on electrical servomechanisms for the non-mathematical student and technician. There is a considerable need for elementary and intermediate books on this subject, which has produced its own jargon, mathematics, and an exclusiveness reminiscent of the ancient religions. Unfortunately, the quality of the book is rather variable: the text is, in places, misleading (witness the opening sentence), and the line diagrams are often incomplete and inadequately captioned. Nevertheless, it is the only book available at this level and so may merit the attention of the interested student.

The book opens with an introductory section describing the need for servo systems, their general form, and the basic response to step-functions and basic components.

Chapter two is on system response, and might well have been placed later in the book, when the student reader would have become more familiar with components and terms. Further, it could well have been much larger and wider in scope. In view of the importance of the response of servomechanisms, the paucity of information here must be regarded as a serious shortcoming, despite the limitations of a maths-free text. Stability, Nyquist and Bode criteria, open loop frequency and phase responses, each of which may be well understood without recourse to the calculus, are completely absent. Indeed, the root of the subject receives no attention.

Similar omissions occur in the following chapters. Chapter three, on error detectors, completely omits mention of control transformers, probably the most important single type of error detector. These are held over to a short section in the lengthy following chapter on synchros, which, incidentally, is somewhat inadequately illustrated.

The subsequent chapters cover DC/AC aspects, modulators and demodulators, magnetic amplifiers, thermionic amplifiers, analogue computing, low power motors, etc., rotating amplifiers, thyatron control and transistors in that disorder, some being sketchy and others adequate.

The overall impression is of a somewhat confused collection of sketches on the subject, notable for the omissions, poor diagrams and an inexcusably incomplete bibliography, there being no reference to J. C. West, Hammond, nor Chestnut and Meyer, each of which can offer further good reading to the intelligent student, despite the mathematics. With regard to illustrations, even some good plates of commercial origin would have been welcome. Surely, in a book of this price, some half-tone plates could be provided. Moreover only one set of circuit diagrams shows any typical values of component, current, voltage or the like. Also a glossary would not be out of place in a book of this sort.

Nevertheless, the authors and publishers are to be congratulated on tackling this field, and we look forward to the second edition.

**THE
MARCONI REVIEW**

JANUARY 1959 — DECEMBER 1959

VOLUME XXII NOS. 132 — 135

INDEX

VOLUME XXII NOS. 132 — 135

	<i>Issue</i>	<i>Page</i>
A utomatic Direction Finders, Some Factors in the Design of VHF	135	168
Automatic Plotter, The Marconi	135	215
B eam Aerials for Long Distance Telecommunications— Foreword	133	73
Band-pass Filters in Waveguides, The Design of	133	99
B ook Reviews		
Analysis of Linear Systems	135	241
Analytical Transients	135	244
Basic Electricity—in five volumes	135	241
Basic Mathematics for Radio and Electronics	132	72
Bibliographia Marconiana	132	36
Cathode Ray Tube and its Applications, The Einschwingvorgange in der Nachrichten Technik (Transient Response in Communication Technique)	135	243
First Course in Television	132	17
Frequency Modulation	132	71
Metal Rectifying Engineering	135	243
Physics and Mathematics in Electrical Communications	134	164
Practical Hi-Fi Handbook	134	163
Principles of Transistor Circuits	134	153
Radio Engineering Formulae and Calculations	133	98
Telecommunication Principles	132	71
Television Servicing	135	233
D irection Finding—Foreword	135	165
Direction Finders, Bearing Errors in Medium Frequency Automatic	135	225
Direction Finders, Some Factors in the Design of VHF Automatic	135	168
Direction Finders, A Method of Providing Test Signals of Calculable Strength for Airborne Radio	135	234
Direction Finders, Operational Applications of VHF	135	199

	<i>Issue</i>	<i>Page</i>
E lectro-mechanical Filters, A Theoretical Analysis of the Torsional	134	119
E lectro-mechanical Filter, The Practical	134	144
F errites at X-band Frequencies, Apparatus for the Measurement of Tensor Permeability and the Dielectric Properties of	134	154
F ilter Developments. Recent—Foreword	134	117
F ilters in Waveguides, The Design of Band-pass Filter, The Practical Electro-mechanical	133	99
F ilters, A Theoretical Analysis of the Torsional Electro-mechanical	134	144
F ilters, A Theoretical Analysis of the Torsional Electro-mechanical	134	119
L ine Deflection Circuits for Television, Transistor	132	38
M etallurgy of Semiconductors, in particular Germanium and Silicon	132	3
P lotter. The Marconi Automatic	135	215
S emiconductors, in particular Germanium and Silicon, Metallurgy of	132	3
S ilicon Single Crystals, The Effects of Seed Rotation on Properties of	132	18
T elevision, Transistor Line Deflection Circuits for	132	38
T est Signals of Calculable Strength for Airborne Radio Direction Finders, A Method of Providing	135	234
T ransistors—Foreword	132	1
T ransistor Line Deflection Circuits for Television	132	38
T ransmission of Electro-magnetic Waves through Wire Gratings (experimental)	133	91
T ransmission of Electro-magnetic Waves through Wire Gratings (theory)	133	77
W ire Gratings (experimental), Transmission of Electro-magnetic Waves through	133	91
W ire Gratings (theory), Transmission of Electro-magnetic Waves through	133	77

*Designed by London Typographical Designers Limited
Printed by Kelihier, Hudson & Kearns Limited, London, England.*

THE
MARCONI REVIEW

JANUARY 1960—DECEMBER 1960

VOLUME XXIII NOS. 136—139

INDEX

VOLUME XXIII NOS. 136—139

	<i>Issue</i>	<i>Page</i>
Aerial Calibration by Solar Noise, using Polar Display	136	33
Aerial Design, The Application of "Deuce" to a Problem in	138	104
Aerial Investigations using Natural Noise Sources	136	2
Aerial Papers in this Issue, The — (Foreword)	136	1
Book Reviews		
An Approach of Electrical Science	136	50
Circuit Theory of Linear Noise Networks	138	139
Experimental Radio Engineering	136	47
Fundamentals of Radio Telemetry	136	49
Guide Technique de l'Electronique Professionnelle	136	47
Linear Network Analysis	136	49
Principles and Practice of Radar (Sixth Edition)	136	46
Principles of Frequency Modulation	136	48
Principles of Servomechanisms	139	204
Radio and Electronic Components Vols. 3 and 4	136	52
Radio and Electronics	137	98
Radio Circuits	136	47
Radio Engineering Handbook	136	44
The Services Textbook of Radio Vol. 5	137	99
Transmission Circuits	137	100
Two-Way Radio	136	51
Conversion System for the Production of Bright Radar Displays, An Experimental Radar	139	184
"Deuce" Computer in Technical Problems, Some of the Uses of the — (Foreword)	138	101
"Deuce" Computer to Network Design, An Application of the	138	140
"Deuce" to a Problem in Aerial Design, The Application of	138	104
Diffraction Round a Sphere or Cylinder, A Note on	139	170
Digital Discs, A Method of Production of High Accuracy	137	65

	<i>Issue</i>	<i>Page</i>
E rrors on the Polar Diagram of a Slot Array. The Effects of	138	110
I nsertion-Loss Equalization, with a Digital Computer	138	149
N etworks, A Modified Synthesis Procedure for Two-Terminal Pair	137	59
N etworks with Prescribed Delay and Amplitude Characteristics, Design of	138	115
N oise Sources. Aerial Investigations using Natural	136	2
N oisy Signals. The Effects of Mixing Two	139	153
R adar Aerials, using Stellar Noise, Some Measurements on	136	21
R adar Conversion System for the Production of Bright Radar Displays, An Experimental	139	184
R eceiver Performance under Operational Conditions, The Monitoring of	137	53
S lot Array. The Effects of Errors on the Polar Diagram of a	138	110
S tellar Noise. Some Measurements on Radar Aerials, using	136	21
S olar Noise. using Polar Display. Aerial Calibration by	136	33
W avemeter Design, High Q	137	85